Renewable and Sustainable Energy Reviews 180 (2023) 113306

Contents lists available at ScienceDirect

Renewable and Sustainable Energy Reviews

journal homepage: www.elsevier.com/locate/rser

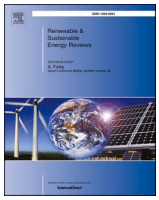

Green roofs as a nature-based solution for improving urban sustainability: Progress and perspectives

Giouli Mihalakakou [a], Manolis Souliotis [b,*], Maria Papadaki [c], Penelope Menounou [a], Panayotis Dimopoulos [d], Dionysia Kolokotsa [e], John A. Paravantis [f], Aris Tsangrassoulis [g], Giorgos Panaras [h], Evangelos Giannakopoulos [i], Spiros Papaefthimiou [j]

[a] Department of Mechanical Engineering and Aeronautics, University of Patras, Greece
[b] Department of Chemical Engineering, University of Western Macedonia, Greece
[c] Department of Environmental Engineering, University of Patras, Greece
[d] Laboratory of Botany, Division of Plant Biology, Department of Biology, University of Patras, Greece
[e] School of Chemical and Environmental Engineering, Technical University of Crete, Greece
[f] Department of International and European Studies, University of Piraeus, Greece
[g] Department of Architecture, University of Thessaly, Greece
[h] Department of Mechanical Engineering, University of Western Macedonia, Greece
[i] Department Biosystems and Agricultural Engineering, University of Patras, Greece
[j] School of Production Engineering and Management, Technical University of Crete, Greece

ARTICLE INFO

Keywords:
Modeling of green roofs
Experimental studies of green roofs
Energy and environmental benefits of green roofs
Noise reduction of green roofs
Life cycle assessment of green roofs

ABSTRACT

Green roofs are artificial ecosystems that provide a nature-based solution to environmental challenges such as climate change and the urban heat island. Green roofs aid in the conservation of both cooling and heating energy; deposition of particulates and mitigation of air pollution; control of runoff and water pollution; promotion of biodiversity; and provision of aesthetic and health benefits. This research is a holistic review of the green roof literature and provides a global perspective of the subject with a classification of modelling studies; and an extensive review of contributions to energy conservation, carbon sequestration, mitigation of air pollutants, runoff control; and urban noise reduction. The review covers the system's thermal performance modelling through several methodologies; experimental studies; parametric studies to assess the impact of various parameters on the system's energy efficiency using several configuration parameters such as leaf area, foliage height and density, plant coverage, roof insulation, soil thickness, and irrigation; energy benefits; and environmental benefits including air pollutants mitigation, carbon sequestration, runoff control and urban noise reduction. Finally, review was complemented with a life cycle assessment study of green roofs, which examined the extraction of raw materials, manufacturing and construction, transportation, and disposal.

Green roofs can reduce the cooling load by up to 70%, decrease the indoor temperature achieving an indoor air temperature reduction up to 15 °C, and provide a significant improvement of thermal comfort conditions. The environmental benefits of green roofs were focused on decreasing pollutants concentrations (e.g. $PM_{2.5}$, PM_{10}, O_3, NO_2), sequestering carbon and reducing urban noise.

1. Introduction

Urban sustainability has become one of the greatest challenges during the last few decades, as climate change, anthropogenic activities, and increased urbanization have resulted in a number of negative environmental consequences such as global warming, air pollution, stratospheric ozone depletion, the Urban Heat Island (UHI) effect, excessive noise, and a decline in biodiversity decrease [1–3], contributing to a degradation of human mental, psychological and physical health [4]. To mitigate these issues, many sustainable approaches, nature-based solutions, practices, methodologies, and algorithms have been designed and implemented, including energy efficient buildings, use of renewable energy sources, air and water pollution mitigation techniques, urban green spaces, an expansion of green infrastructure, etc. [5,6]. Nature-based solutions include mitigation and adaptation

* Corresponding author.
E-mail address: msouliotis@uowm.gr (M. Souliotis).

https://doi.org/10.1016/j.rser.2023.113306
Received 17 November 2022; Received in revised form 7 April 2023; Accepted 18 April 2023
Available online 25 April 2023

List of abbreviation

ADP	Abiotic depletion potential
ANN	Artificial Neural Networks
CBA	coal bottom ash
DAI	Dissolved Aluminum
EGR	Extensive Green Roof
EN	European Norm
FAAs	fly ash-based aggregates
GR	Green Roof or Green Roofs
GR-a:	alternative green roof
GR-c:	conventional green roof
GRWRS	Green roof and water reuse system
GWP	Global warming potential
HMW	hydrophilic mineral wool
HVAC	Heating, Ventilation, and Air Conditioning
IGR	Intensive Green Roof
LAI	Leaf Area Index
LAD	Leaf Area Density
LCA	Life Cycle Assessment
LCIA	Life Cycle Inventory Analysis
LDPE	Polyethylene
ODP	Ozone depletion potential
PMV	Predicted Mean Vote
POCP	Photochemical ozone creation
SIGR	Semi-Intensive Green Roof
TGBR	Traditional Gravel Ballasted Roof
THR	Traditional Horizontal Roof
TOC	Total Organic Carbon
WRR	White Reflective Roof

strategies primarily aimed at creating and maintaining a balance between biotic and abiotic ecosystem components by enhancing biodiversity, expanding green infrastructure, and supporting the sustainability transition of cities by creating a livable built environment [7–12]. Mitigation and adaptation strategies and techniques, which include the significant increase of green areas as well the exploitation of natural heat sinks such as ground, sky, and water for excessive heat dissipation [13–16], are challenging to implement in the urban areas due to augmented urbanization, a phenomenon that results in a dramatically increased demand for buildings, space, water, and energy, thereby exerting pressure onto rural lands, which are predicted to shrink by 30%, affecting livability [17,18]. Thus, considering that rooftops in urban areas are primarily unused impervious surfaces, the green roof technology, a widely documented, technical, and nature-based solution for improving sustainability in the built environment, has been applied to increase building energy efficiency, but also to achieve many environmental, aesthetic, psychological, physiological, and economic benefits able to transform an aesthetically indifferent space like a rooftop into a viable, multi-functional and sustainable area using soil, vegetation, and plants [19–21].

Green roofs (GR) are designed and implemented as artificial ecosystems that improve urban sustainability by performing numerous functions and providing a vast array of interacting services and benefits at various scales [22–24]. Thus, the scientific literature of the last few decades has revealed a remarkable number of associated benefits spanning a broad range of sustainability areas and making GR a popular engineering application worldwide for combating climate change, mitigating UHI, and improving urban air and water quality. The benefits offered by GR can be categorized as follows [17,25]:

(a) *Energy benefits*: numerous theoretical and experimental studies have assessed the energy conservation potential of GR systems [26–33]. Energy benefits directly expressed through the reduction of the cooling and heating load depend strongly on building characteristics and heat transfer processes, which are primarily determined by the U-values of roof components. Moreover, climate type, system configuration parameters and especially plant canopy characteristics as expressed by the Leaf Area Index (LAI), which influence shading, evapotranspiration, and latent and convective heat fluxes, have a significant effect on the energy behavior of a system [31,34–36].
(b) *Environmental benefits and air quality*: green infrastructure, including GRs, contribute to air pollutant deposition enhancement to vegetated areas, thus reducing their concentrations and purifying the air [37,38], as well as to carbon dioxide (CO_2) concentration reduction primarily due to reduced building energy consumption through evapotranspiration and also because plants and vegetation absorb significant quantities of CO_2 through photosynthesis [39].
(c) *Environmental benefits and water quality*: vegetated roofs present a significant regulating effect on runoff water volume, thereby contributing to pluvial flood mitigation as well as runoff water quality improvement and to the reduced presence of urban stormwater pollutants as plants and the soil substrate absorb and filter pollutants and act as sinks for nitrate and ammonia nitrogen [40–42].
(d) *Ecosystem benefits*: GR can provide important ecosystem services for urban sustainability primarily related to an increase in biodiversity and the renaturing of cities [43,44].
(e) *Social-aesthetic and psychological benefits*: GR could provide a refuge of peace and tranquility in the heart of urban environment with less noise and pollution, thereby contributing to psychological, physical health, and well-being improvements [4].

This article is primarily a bibliographic review of the scientific processes, models, and optimization methods that describe the thermal performance of a GR system holistically, as well as system benefits. The review covers the following topics: (i) old and recent advances and trends in green roof scientific data from different disciplines; (ii) modeling system thermal performance with a focus on the type of model assumptions and experimental validation; (iii) parametric studies to assess the impact of system configuration parameters on thermal efficiency; and (iv) case studies and data collected from applications at different scales, including a description of system benefits and an evaluation of environmental impacts through life cycle assessment.

The novel aspects of this research may be summarized as follows:

(a) It provides a comprehensive critical perspective of the thermal performance modeling of GRs, classifying theoretical approaches according to the underlying fundamental scientific principles. Model presentation is enriched with an extensive review of parametric studies, thereby examining the effect of the configuration parameters of the main system on its energy performance and thermal fluxes.
(b) It offers a critical presentation of the most important findings regarding the benefits of energy systems, mentioning concurrently the most significant problems, limitations, and assumptions.
(c) It reviews the most notable contributions of GRs to air quality improvement, combining carbon sequestration through photosynthesis with pollutant concentration reduction through evapotranspiration and deposition processes, as well as significant GR contributions to the improvement of runoff water quality.

(d) Finally, in addition to reviewing the aforementioned GR research topics and activities, it outlines future scientific directions of system engineering applications, providing a comprehensive view of research advancements.

The article is structured as follows: Section 2 presents the main modeling approaches used to describe the thermal performance of a GR system as well as an analytical parametric study illustrating the impact of the main system parameters on its efficiency. A GR benefits presentation is also included, highlighting research progress in system energy, environmental and noise reduction (Sections 3, 4, and 5, respectively). The holistic approach of this research is concluded with: (a) a Life Cycle Assessment (LCA) review, (Section 6), (b) an analysis of plants selection and water scarcity issue (Section 7), and (c) engineering applications subjects (Section 8).

2. Attributes and processes

In recent decades, many GR applications have been documented and may be categorized into three primary groups [19,41]: (a) *extensive* [20,21,50], identified as one of the most efficient solutions to implement sustainability in the building sector, characterized by shallow soil depth (less than 20 cm) and vegetation (e.g. short plants, grasses, herbs, short-grasses and mosses) requiring little maintenance and no permanent irrigation system, which could be considered a cost effective system; (b) *simple* or *semi-intensive* [5,19,22], characterized by small plants, grasses, lawns, and small shrubs, requiring moderate maintenance and occasional irrigation; and (c) *intensive* [18,19,23], characterized by deep substrates reaching a depth of 1 m, capable of supporting bigger plants such as large shrubs, grassland, flowerbeds, and even trees, requiring systematic maintenance and irrigation.

GRs are not designed and implemented as conventional roof gardens, but rather as engineering structures consisting of the following components [22,23,49]:

(1) *Vegetation*: plants play an important role in improving air and runoff quality [50,51] as well as conserving energy [26].
(2) *Soil layer*: the growth substrate characteristics are crucial GR parameters [52].
(3) *Filter layer*: separates soil and drainage material [53].
(4) *Drainage material*: provides the necessary balance between air and water systems and improves the thermal characteristics of GRs [50].
(5) *Root barrier*: prevents roof structure damage by plant roots [54].
(6) *Waterproofing layer*: is the most essential component for GR protection [54].

The filter layer and the drainage material could be considered the GR support layer, whereas the root barrier and the waterproof layer could be considered the insulation layer [55]. Fig. 1 illustrates the layers of a typical GR [56].

Section 2 consists primarily of the main modeling approaches describing the thermal performance of GR system (sub-section 2.1), and secondly of an analytical parametric study demonstrating the impact of the main system parameters on its efficiency, (sub-section 2.2).

2.1. Modeling the thermal performance of a green roof system

As depicted in Fig. 2, thermal processes in GRs are rather complex, dynamic, and interactive phenomena, involving several dominant mechanisms that are strongly related to GR components. These components succeed in providing a unique thermal material capable of combining different and interactive thermal processes, such as conduction; convection; evapotranspiration and evaporative cooling; radiative cooling; shading; thermal storage, etc. [55].

The aforementioned thermal processes can be summarized as follows in relation to their respective GR components:

(a) GRs support the *structure layer* (including all layers from the bottom to the soil layer): their material is regarded as solid and heat transfer can be described using the Carslaw and Jaeger conductional processes [57,58].
(b) The *soil layer* is a complex medium consisting of both solid state and fluid components (mainly water, air, and water-vapor). In

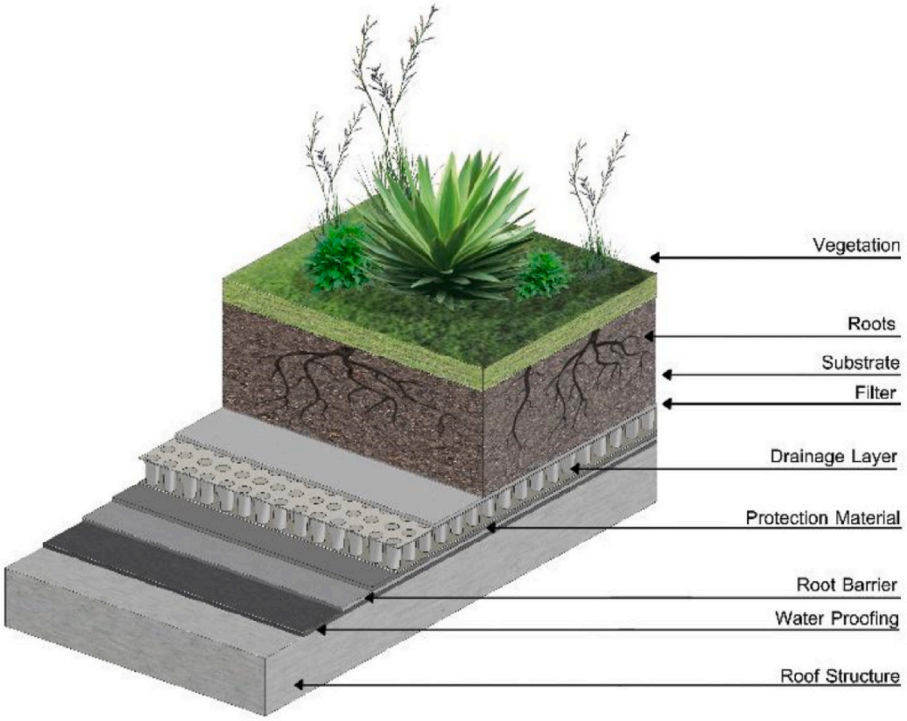

Fig. 1. Typical green roof layers [56].

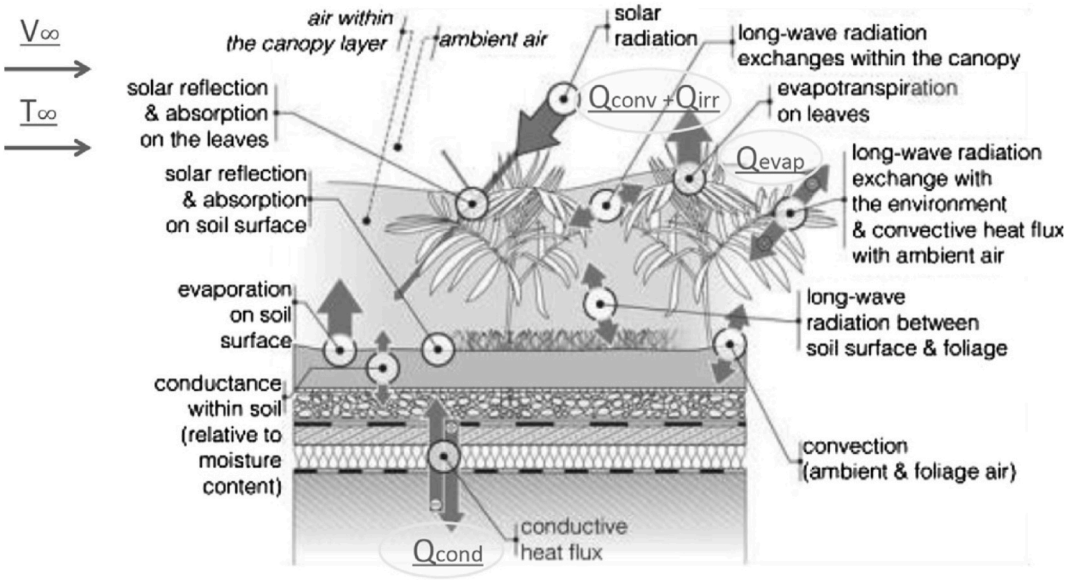

Fig. 2. Heat transfer processes in green roofs [19].

solids, conduction is the predominant heat transfer mechanism, while convection is predominant in fluids (sensible heat flux). Latent heat transfer due to water evaporation (latent heat flux) should be considered, as evaporative cooling would contribute significantly to GR energy performance, while simultaneous heat and mass transfer due to soil moisture migration should not be disregarded [31,58,59]. Also, long-wave radiation exchange between the soil surface, foliage, and ambient air may play a significant role in the thermal behavior of GRs, particularly under clear sky conditions, when the atmospheric window operates effectively and radiative cooling can be achieved via the GR system [52]. Due to its high thermal capacity and time lag effect, soil is also capable of functioning as a thermal storage mass [19].

(c) The *canopy layer* (consisting of foliage and ambient air) is very significant because of its impact on the mitigation of the UHI and is characterized and influenced by many environmental parameters and thermal processes, such as: (1) solar radiation absorbed by the foliage; (2) long-wave radiation emitted by foliage into the ambient air and exchanged between the foliage and the air as well as the soil; (3) convective heat transfer phenomena occurring between the air and the foliage as well as between the soil surface and the ambient air of the canopy layer; (4) evapotranspiration and shading occurring in the foliage [60]; and (5) convective heat transfer phenomena between the canopy and the ambient air [19,31,58,61].

Modeling of GRs is challenging because it involves sensible and latent heat exchange as well as all the heat transfer phenomena shown in Fig. 2. In order to assess and predict the thermal and energy balance of GRs, different modeling approaches have been developed over the past few decades. In this research, models are classified into three groups: (a) based on improving the thermal transmittance coefficient (U-value) through a GR [26–28,30]; (b) based on describing and calculating the energy balance of a GR system [29,31,34,46,58,59,61–70]; and (c) data-driven models aiming to predict the GR thermal behavior using historical data [32,71,72]. In Table 1 and the following paragraphs, the principal characteristics of the models simulating the thermal performance of a GR system are summarized.

2.1.1. Thermal transmittance coefficient (U-value)

The simplest approach for calculating the thermal performance of a GR system consisted of its representation by a proportional reduction of the U-value coefficient. Niachou et al. [26] presented an analysis of the thermal performance of a GR system and its significant reduction of the cooling load reduction of buildings, based primarily on the increase in the thermal capacity of the roof and the decrease in heat losses. Consequently, those authors provided an extensive evaluation of the thermal properties of GR systems by conducting experiments and developing mathematical models. Those authors estimated the thermal transmittance coefficients of various types of roofs constructed from different materials, over which a GR was installed; the building energy performance was simulated for one year with and without the GR system, resulting in the calculation of the GR's contribution to the reduction of the cooling load and energy savings. Comparing theoretical to experimental figures, it was determined that the model was sufficiently accurate.

In [27], the effect of a GR system on the energy consumption and cooling load reduction of a hypothetical multi-story commercial building in Singapore was studied and presented. The methodology was based on the thermal resistance coefficient (R-value), and the calculation for each layer of various GRs included various soil and plant types. All types of GRs were coupled with the building and their annual energy performance were simulated using the DOE-2 energy simulation program [73]. Model results were successfully validated against experimental values. Additionally, the U-value method was used in Ref. [25] and in Ref. [27].

2.1.2. Energy balance

The majority of mathematical models describing the thermal performance of GRs are predicated on the expression and calculation of the energy balance of the different components of the system. Numerous mathematical formulations for the energy balance of a GR system have been considerably influenced by two research studies. In the first such study, Palomo del Barrio [58] presented one of the first basic mathematical models calculating the thermal performance during the summer and the cooling effect of a GR system, using simplifications of its transient thermal processes. The model took into account three GR components: (1) structural support layer, (2) soil layer, and (3) canopy layer. For the first component, the author assumed solid homogeneity with constant thermal properties, and the heat transfer process was described by the following one-dimensional heat conduction equation in solids [57]:

Table 1
Main characteristics of models simulating the thermal performance of a GR system.

Reference	Short description	Validation mode
[46]	Based on energy balance calculations. A comprehensive energy budget description taking into account photosynthetic processes during plant respiration.	Authors conducted extensive experimental investigations to validate model accuracy.
[26]	Based on U-value coefficient calculations.	Experimental data were compared to theoretical results, and the model was determined to be accurate.
[31]	Authors calculated the energy balance equations for two GR layer-components, namely foliage and soil. Based on [61].	Author model was based on [61], which was validated successfully.
[58]	One of the earliest transient, numerical models to calculate the GR energy balance for the structural, soil, and canopy layers.	Authors made no mention of a validation process.
[59]	Authors took into account the primary heat and mass transfer processes. Based on [61].	Author model was based on [61], which was validated successfully.
[61]	One of the most comprehensive, straightforward and concise energy balance-based approaches in the scientific literature. It has been used extensively by several researchers.	The model was validated successfully against an comprehensive set of measurements.
[62]	Based on energy balance. Authors emphasized the importance of evapotranspiration.	Model results were validated successfully against experimental values.
[32]	Data-driven. An ANN model predicted that a GR system would reduce the cooling load.	Model results were found accurate against numerous experimental values.
[71]	Data-driven. An ANN model predicted the mitigating effect of a GR system on the UHI.	Urban characteristics and morphology parameters generated from satellite photos and light detection and ranging data were used to train and evaluate the outputs of ANNs.
[72]	Data-driven. An ANN approach for estimating the GR impact on the winter warming effect.	The ANN model was trained and tested using experimental values, and it was determined to be accurate.
[34]	Based mainly on [58] and an energy balance. A transient, numerical mathematical model was solved using the finite-volume method.	The model was thoroughly validated against experimental data and determined to be sufficiently accurate.
[63]	Based on energy balance and the principles of heat and mass transfer.	The accuracy of the model was determined by experimental validation.
[64]	Based on energy balance. One-dimensional, transient model incorporating both biotic and abiotic GR components.	It was determined that the model was sufficiently accurate after comparing theoretical results to an extensive set of experimental data.
[65]	Based mainly on [61] and an energy balance. Using the principles of evaporative cooling, a water balance model was created and connected with a thermal model.	Authors presented a comprehensive analysis and validation of experimental data.
[29]	Based on energy balance. A transient, one-dimensional model that describes heat and mass transfer processes in the structure, air, soil, and canopy.	Model was successfully validated against literature results.
[66]	Based on energy balance. Photosynthesis and evapotranspiration processes of the plants were also considered. Finite differences were used to solve differential equations numerically.	Successfully validated against experimental data.
[67]	Based mainly on [61].	Model results presented in Ref. [61] were successfully validated.
[68]	Based on energy balance. One-dimensional model that calculated heat and mass transfer processes in plants, soil, and structure layers.	Model results were validated successfully against experimental data.
[69]	Based on energy balance. Authors used heterogeneous materials in each GR layer.	Model results were validated successfully against literature and experimental data [46].
[70]	Based on energy balance. Using highly nonlinear differential equations, the finite-differences method was used to numerically and explicitly solve heat and mass transfer processes.	Multiple test cases, including the canopy and soil layers, as well as a realistic multi-layered GR system were used to validate the model.
[27]	Based on R-value coefficient calculations.	Model results were validated successfully against experimental values.
[28]	Based on U-value coefficient calculations.	The model was validated successfully against experimental data.
[30]	Based on U-value coefficient calculations and on [27,28].	The models presented in Refs. [27,28] were validated successfully using experimental data.

$$\rho \bullet C_p \frac{\partial T_s(z,t)}{\partial t} = \lambda_s \frac{\partial^2 T_s(z,t)}{\partial t^2} \tag{1}$$

where $T_s(z,t)$ represents the temperature field, ρ the density, C_p the specific heat, and λ_s the thermal conductivity of the material.

The soil is considered to be a porous medium with three phases: solid, liquid (water), and gas. Thus, heat transfer mechanisms were expressed as sensible and latent heat via conduction in solids and convection in fluids. Temperature differences in the soil result in a simultaneous migration of soil moisture, which is caused by heat transfer. Consequently, simultaneous heat and mass transfer processes in the soil were described by a set of coupled, one dimensional, transient differential equations with two dependent variables, temperature and moisture content:

$$\rho \bullet C_p(\omega,T)\frac{\partial T(z,t)}{\partial t} = \frac{\partial}{\partial z}\left\{[\lambda(\omega,T) + \Lambda \bullet D_{vT}(\omega,T)]\frac{\partial T(z,t)}{\partial z} + \Lambda \bullet D_{vw}(\omega,T)\frac{\partial \omega(z,t)}{\partial z}\right\} \tag{2}$$

$$\frac{\partial \omega(z,t)}{\partial t} = \frac{\partial}{\partial z}\left\{D_w(\omega,T)\frac{\partial \omega(z,t)}{\partial z} + D_T(\omega,T)\frac{\partial T(z,t)}{\partial z}\right\} - \frac{\partial K(z,t)}{\partial z} + \varphi(z,t) \tag{3}$$

where

$T(z,t)$: local temperature in the porous medium domain (°C)

$\omega(z,t)$: local volumetric moisture content in the porous medium domain (−)

$\rho \bullet C_p(\omega,t)$: weighted heat capacity ($J \cdot kg^{-1} \cdot K^{-1}$)

$\lambda(\omega,t)$: effective thermal conductivity ($W \cdot m^{-1}$)

Λ: latent heat of vaporization ($J \cdot kg^{-1}$)

$D_{vT}(\omega, T)$: non-isothermal vapor diffusivity coefficient ($kg \cdot m^2 \cdot s^{-1} \cdot K^{-1}$)

$D_{vw}(\omega,T)$: isothermal vapor diffusivity coefficient ($kg \cdot m^2 \cdot s^{-1} \cdot K^{-1}$)

$D_w(\omega,T)$: isothermal mass (vapor and liquid) diffusivity coefficient ($m^2 \cdot s^{-1}$)

$D_T(\omega,T)$: non-isothermal mass (vapor and liquid) diffusivity coefficient ($m^2 \cdot s^{-1} \cdot K^{-1}$)

$K(z,t)$: hydraulic conductivity ($m \cdot s^{-1}$)

$\varphi(z,t)$: water sink representing the root extraction term (s^{-1}).

The canopy model was based on several thermal processes, including heat and mass transfer, with the following being the most important: (a) solar radiation absorbed by the foliage; (b) convective processes between the soil surface and the canopy air, between the foliage and the canopy air, and between air in the canopy and the free air; (c) evapotranspiration in foliage; (d) evaporation/condensation at the soil surface; and (e) long-wave radiation exchanges between the leaves, the soil surface, the sky, and in the foliage. Thus, the energy and vapor balance equation was expressed as follows:

$$\left.\begin{aligned}(\rho \bullet C)_p \bullet dLAI\frac{dT_p}{\partial t} &= \varphi_{rad,sol} + \varphi_{rad,TIR} + \varphi_{trans,p-a}\\ (\rho \bullet C)_a \bullet L\frac{dT_a}{\partial t} &= \varphi_{conv,a-p} + \varphi_{con,a-g} + \varphi_{conv,a-\infty}\\ \rho \bullet a \bullet L\frac{d\theta_a}{\partial t} &= \varphi_{vap,a-p} + \varphi_{vap,a-g} + \varphi_{vap,a-\infty}\end{aligned}\right\} \quad (4)$$

where

T_p: leaf temperature (average in the control volume) (K)
T_a: air temperature (average in the control volume) (K)
θ_a: air specific humidity (average in the control volume) (kg^{-1})
$(\rho \bullet C)_p$: leaf specific thermal capacity ($J{\cdot}m^{-3}{\cdot}K^{-1}$)
d: average leaf thickness (m)
$(\rho \bullet C)_a$: air specific thermal capacity ($J{\cdot}m^{-3}{\cdot}K^{-1}$)
ρ_a: air density ($kg{\cdot}m^{-3}$)
L: canopy layer thickness (m)
$\varphi_{rad,sol}$: solar radiation absorbed by leaves ($W{\cdot}m^{-2}$)
$\varphi_{rad,TIR}$: net thermal radiation flux on leaves ($W{\cdot}m^{-2}$)
$\varphi_{conv,p-a}$: sensible heat flux between the foliage and the canopy air ($W{\cdot}m^{-2}$)
$\varphi_{trans,p-a}$: energy flux due to leaf transpiration ($W{\cdot}m^{-2}$)
$\varphi_{conv,a-p}$: sensible heat flux between the canopy air and the foliage ($\varphi_{conv,a-p} = -\varphi_{conv,p-a}$) ($W{\cdot}m^{-2}$)
$\varphi_{conv,a-g}$: sensible heat flux between the canopy air and the ground surface ($W{\cdot}m^{-2}$)
$\varphi_{conv,a-\infty}$: sensible heat flux between the canopy air and the outdoor air ($W{\cdot}m^{-2}$)
$\varphi_{vap,a-p}$: vapor flux between the canopy air and the foliage ($kg{\cdot}m^{-2}$)
$\varphi_{vap,a-g}$: vapor flux between the canopy air and the ground surface ($kg{\cdot}m^{-2}$)
$\varphi_{vap,a-\infty}$: vapor flux between the canopy air and the outdoor air ($kg{\cdot}m^{-2}$).

In addition to the three energy balance formulations mentioned previously (support, soil, and canopy), the authors proposed two coupling models based on the heat flux continuity equation at each interface as real boundary conditions at the two interfaces, (support-soil, and soil-canopy). Numerical analysis with the finite volume method was used for discretizing and solving the differential equations. Furthermore, an comprehensive sensitivity analysis with numerous examined parameters was offered.

The second influential study describing the thermal behavior of GRs using a comprehensive, clear, and concise mathematical model [61]. The model was completely developed and implemented inside the EnergyPlus buildings simulation program [74] and has been used extensively by various researchers for parametric studies and experimental validation. This model is based on the energy balance of a typical GR, which is primarily influenced by the following environmental parameters: absorbed solar radiation; sensible heat from convective processes in the soil and plants; latent heat from evapotranspiration; heat transfer from conductional processes in the soil; and long wave radiation exchanges between soil and foliage. Taking into account these parameters, two energy budgets were developed: one for the foliage layer, which was expressed as follows:

$$F_f = \sigma_f\left[I_s^{\downarrow}(1-a_f) + \varepsilon_f I_{ir}^{\downarrow} - \varepsilon_f \sigma T_f^4\right] + \frac{\sigma_f \varepsilon_g \varepsilon_f \sigma}{\varepsilon_1}\left(T_g^4 - T_f^4\right) + H_f + L_f \quad (5)$$

and a second one for the soil surface, which was described as follows:

$$F_g = (1-\sigma_f)\left[I_s^{\downarrow}(1-a_g) + \varepsilon_g I_{ir}^{\downarrow} - \varepsilon_g T_g^4\right] - \frac{\sigma_f \varepsilon_g \varepsilon_f \sigma}{\varepsilon_1}\left(T_g^4 - T_f^4\right) + H_g + L_g + K_v \times \frac{\partial T_g}{\partial z} \quad (6)$$

where

a_f: albedo (short-wave reflectivity) of the canopy
a_g: albedo (short-wave reflectivity) of the ground surface
ε_1: $\varepsilon_g + \varepsilon_f - \varepsilon_f \varepsilon_g$
ε_f: emissivity of the canopy
ε_g: emissivity of the ground surface
F_f: net heat flux to foliage layer (W/m^2)
F_g: net heat flux to ground surface (W/m^2)
H_f: foliage sensible heat flux (W/m^2)
H_g: ground sensible heat flux (W/m^2)
$I_s^{\downarrow}$: total incoming short-wave radiation (W/m^2)
$I_{ir}^{\downarrow}$: total incoming long-wave radiation (W/m^2)
K_v: von Karmen constant (0.4)
L_f: foliage latent heat flux (W/m^2)
L_g: ground latent heat flux (W/m^2)
T_f: foliage temperature (K)
T_g: ground surface temperature (K)
σ: Stefan-Boltzmann constant ($5.67 \times 10^{-8} W/m^2{\cdot}K^4$)
σ_f: fractional vegetation coverage.

Using heat transfer analysis and empirical formulas, sensible (convective) and latent (evaporative) heat fluxes were calculated for both layers, and final equations were linearized and solved within the EnergyPlus program. A comprehensive set of experimental data was used to test and successfully validate model results. Finally, a sensitivity analysis was conducted to conclude that research. Models [58,61] have been cited and used extensively in the scientific literature. To evaluate the cooling potential of a GR system [31], considered the basic algorithms of [58], whereas [28,59,65,67] were significantly influenced by Ref. [61].

The following may also be classified as models based on the development and calculation of GR energy balances. Initially [62], presented a numerical model for predicting the cooling effect and potential of GR systems was presented in. To estimate the energy performance of a building equipped with a GR, the model was developed inside the TRNSYS building simulation environment. Those authors highlighted the importance of evapotranspiration in reducing cooling loads, while their predictive module relied heavily on empirical and semi-empirical formulas from the scientific literature to calculate latent heat fluxes due to evapotranspiration. Model results were successfully validated against experimental values.

Alexandri and Jones [29] developed a one-dimensional transient model with variable humidity that describes heat and mass transfer processes in the structure, air, soil, and canopy of a GR system. Model results were validated extensively and successfully against experimental data. Feng et al. [46] presented and analyzed a significant method for modeling the energy balance in extensive GRs. According to those authors, the energy income and balance equation for an extensive green roof may be expressed as follows:

$$q_{sr} + q_{lr} + q_{cv} + q_{em} + q_{tp} + q_{ep} + q_{sp} + q_{ss} + q_{tf} + q_{ps} + q_{rp} = 0 \quad (7)$$

where q_{sr} is the heat gain from solar radiation, q_{lr} is the heat gain from long-wave radiation, q_{cv} is the sensible heat transferred by convection, q_{em} is the emitted heat loss, q_{tp} is the heat loss due to transpiration, q_{ep} is the heat loss due to evaporation, q_{sp} is the heat stored by plants, q_{ss} is the

heat stored by the soil, q_{tf} is the heat transferred into the building, q_{ps} is the solar heat converted by photosynthesis, and q_{rp} is the heat generated by plant respiration. In order to calculate the energy balance for this model, only eight environmental parameters were required: incident solar radiation, ambient air temperature, dew point, wind velocity above the canopy, soil moisture content, foliage temperature, soil temperature, and the heat transferred into the building beneath. Extensive experimental studies were conducted and accurate theoretical results were reached.

Using Newton's cooling law [75], Ayata et al. [63] calculated the energy balance and sensible heat fluxes in a GR. The following equation was used to estimate an energy balance and associated heat fluxes:

$$R_n - G - L - H = 0 \tag{8}$$

where R_n represents the net radiation, G represents the soil heat flux, L represents the latent heat flux, and H represents the sensible heat flux. The sensible heat flux was calculated using Newton's cooling law and by modifying the Nusselt number for forced and free convection. That research included an extensive experimental analysis, and the model was successfully validated.

In [64], a one-dimensional mathematical model simulating the thermal performance and the cooling and insulating effects of the abiotic components of GRs (soil, water storage, roof support) was developed and presented. Calculations of heat fluxes at the soil surface accounted for conduction, convection, radiation, and evaporation flows that affect the soil surface temperature. For calculating sensible and latent heat fluxes due to convection and evaporation processes, Newton's cooling law and Penman's modified empirical formulas were used [65,75]. The basic energy balance at the soil surface may be expressed as follows:

$$q_0 + q_{ar} - q_{sr} = q_e + q_c + q_d \tag{9}$$

where q_0 is the solar radiation absorbed by the soil, q_{ar} is the long-wave radiation emitted from the ambient air to the soil, q_{sr} is the long wave radiation emitted from the soil to the sky, q_e is the heat loss due to evaporation, q_c is the heat loss due to convection, and q_d is the conductive heat from the soil surface into the soil. All of the aforementioned factors were expressed using theoretical principles of heat transfer and latent heat fluxes in the atmospheric boundary layer, to develop the model's heat diffusion equations, which were solved numerically using finite differences. It was determined that the model was sufficiently accurate after comparing theoretical results to an extensive set of experimental data. Finally, theoretical and experimental results demonstrated that the abiotic components of a GR contribute significantly to the reduction of the cooling load.

The authors of [66] presented a complex set of heat and mass transfer equations that describe the thermal behavior of a GR system by considering simultaneously the four involved components (air, plants, soil, and structure). The description of heat and mass transfer in plants and the calculation of plant metabolism took into account that the energy balance of plants is dependent on both evapotranspiration and photosynthesis. Finite differences were used to solve differential equations explicitly. When compared to the experimental values of [29], the model was found to be accurate.

Chen et al. [68] developed a simplified one-dimensional mathematical model to estimate the energy potential of a GR system particularly during the design stage. That model took into account the plant layer, the soil, and the structure and was designed to operate in two steps: (a) calculate the energy balance between plants and the soil surface, and (b) calculate the conductional process from the soil surface to the structure. During the first step, all heat fluxes were balanced and calculated in the two layers. For the second step, conductional and diffusion processes described in Ref. [57], assuming two conditions regarding the soil temperature: (i) constant soil temperature at the adiabatic depth, and (ii) agreement with the ambient air temperature at the surface. Model results were successfully validated against experimental values.

Models of GR system assume that layers are composed of homogeneous materials with fixed thermal properties. The authors of [69] used heterogeneous materials with different thermal properties for each individual GR layer. This makes the heat transfer analysis more complicated, with the methodology comprising the following steps: (a) considering that the soil layer consists of two materials, solid and water, while the green layer consists of plants and air; (b) assuming the layers are homogeneous and developing heat transfer equations in terms of average variables; (c) developing a mathematical model consisting of two average equations for each layer (soil-water layer, and plants-air layer); (d) proposing closure relationships to reduce unknown problem variables; (e) estimating a numerical solution based on control volumes; and (f) conducting validation. All in all, model results were validated successfully against experimental and published data [46].

In order to evaluate the energy performance of GRs, the authors of [70] developed and presented a transient, numerical, mathematical model based on coupled heat and mass transfer processes through a GR system. Highly nonlinear differential equations describing heat and moisture transport phenomena in the structural layer, the soil, and the canopy were used to simulate the system. Equations governing heat and mass transfer were developed for the canopy air layer, and for the soil as a porous medium. The initial boundary and interface conditions for temperature and moisture were established, the soil was coupled with the canopy, and the soil was coupled with structure as a boundary element. Using the finite differences method, a set of coupled highly nonlinear differential equations was solved numerically and explicitly. Various test cases, including canopy and soil layers, and a realistic multi-layered GR system were used to validate the model.

2.1.3. Data-driven models

Data-driven models are computing systems based on historical data rather than the mathematical expressions of deterministic models. Artificial Neural Networks (ANNs) are data-driven computational systems that imitate biological neurons and perform learning, predictions, and estimations. Data-driven models rely solely on historical data, which may offer significant benefits such as efficiency (fairly complex nonlinear systems and processes that can be modeled with sufficient accuracy), simplicity (all they require is training and testing with historical data), and computational speed.

Pandey et al. [32] designed and trained a ANN to predict reduction in cooling load caused by a GR system. The ANN architecture consisted of a feed-forward network with multiple layers that was based on a back-propagation algorithm with a 0.1 learning rate coefficient. The training input parameters were the dry bulb temperature values, relative humidity, average solar intensity, and wind speed, while the ANN output was a reduction in heat gain. Many experimental values were used to test the network's performance, and the ANN was found to be sufficiently accurate. The results demonstrated that GR systems can be remarkably effective at reducing summer cooling loads.

Using backpropagation methods, a multilayered feed-forward ANN was designed, trained, and evaluated to estimate the mitigating effect of a GR system on the UHI [71]. The ANN was trained with the help of 2D and 3D urban characteristics and morphology parameters derived from satellite images and light detection and ranging data. It was determined that greening 3.2% of all building rooftops would result in an average decrease of 1.96 °C in soil surface temperature, indicating a substantial achievement in UHI mitigation.

Wei et al. [72] presented an ANN approach for estimating the impact of a GR system on the winter warming effect. Extensive experimental research was conducted in a subtropical climate in China, with three experimental buildings outfitted with GR systems for measuring the Roof Outer Surface Temperature (ROST) in the winter. An ANN was designed and trained with outdoor temperature, relative humidity, wind speed, solar radiation, soil moisture content, and soil layer thickness being the input parameters, and ROST being the output. It was

determined that a genetic algorithm backpropagation ANN model that was trained and tested with experimental values, was accurate. It was shown that a maximum ROST of 13.5 °C could be attained with a 20 cm soil thickness and 3.9% soil moisture content.

Lately, Mazzeo et al. [76], used an artificial intelligence-based approach to develop a forecasting model that predicts the cooling effect of green roofs on buildings and the surrounding area. The model was trained using data from experimental tests and simulations of green roofs' thermal performance under different environmental conditions. The study found that green roofs can significantly reduce the surface temperature of buildings and the surrounding area and improve the buildings' energy efficiency. The authors conclude that the developed forecasting model can help in the design and optimization of green roofs to maximize their potential in mitigating the urban heat island effect and improving building thermal performance in the Mediterranean area. Overall, the article offers valuable insights into the use of green roofs as a sustainable solution to urban heat island effect and energy efficiency in the Mediterranean region.

Many experimental studies have been conducted and presented globally, with the goals of (a) quantifying energy savings and air quality improvement leading to UHI mitigation, and (b) validating the author's mathematical formulations for the thermal performance of the GR system. Table 2 summarizes several representative experimental studies of GR systems, with an emphasis on model validation and energy efficiency quantification.

2.2. Parametric studies

After investigating, analyzing, and modeling the energy performance of a GR system, most researchers have enriched and concluded their studies with sensitivity analyses and parametric studies that primarily investigated the effect of several configuration parameters on the GR system's energy performance and thermal fluxes. Parametric studies have accounted for numerous variables including both system configuration and climatic parameters. Researchers have examined the following system configuration parameters: leaf area index, foliage height and density, plant coverage, roof insulation and insulation layer thickness, soil layer thickness, and irrigation, among others [26,30,31,34–36,58,61,77,81,82]. Among the climatic parameters were absorbed solar radiation, ambient air temperature, air relative humidity, evapotranspiration rate, and wind speed [36,81,83].

According to the scientific literature, one of the most significant system configuration parameters determining the energy performance of a GR system is the Leaf Area Index (LAI), a key structural element that characterizes the plant canopy. LAI is a dimensionless quantity, defined as the ratio of the (one-sided) leaf area to the unit ground surface area [84]. Due to its large contribution to shading and evapotranspiration, a substantial number of researchers cited the LAI among as one of the primary GR system variables impacting the thermal behavior of the system, [34–36,58,61,82,85].

Table 3 summarizes the quantitative findings of many research studies focusing on parametric analyses and using several parameters, including LAI, soil layer thickness, insulation thickness, irrigation, foliage height and density, type of planted roof, plant coverage, etc. The following aspects of these studies are highlighted:

(a) LAI was found to be the most important parameter affecting the thermal behavior of the GR system. An increase in LAI led to a significant reduction in the solar transmittance of the canopy and an improvement in the shading effect, hence reducing the amplitude of temperature fluctuations in the canopy air and the energy demand.
(b) The thickness of the insulation layer may have a significant impact, as its increase reduces the cooling capacity of a system.
(c) An increase in soil thickness leads in greater energy savings because it is considered an additional layer when calculating the U value of the roof.
(d) An increase in GR plant coverage led to a decrease in substrate surface temperature, resulting in a reduction in cooling load and sensible heat flux to the atmosphere.
(e) The influence of foliage height was found to be an important system characteristic only when combined with vegetation density.
(f) The relative humidity of the atmosphere played the most significant influence in determining evapotranspiration.
(g) An increase in wind speed decreased humidity, hence increasing evapotranspiration and the cooling capacity of the system.
(h) Finally, the greatest annual energy savings were achieved for non-insulated buildings equipped with a GR system.

3. Energy benefits and thermal comfort conditions improvement

It is worth noting that 20% of the total urban surface is comprised by roofs, providing a significant benefit for greening space in the urban environment [86–89]. Numerous studies have investigated the role of GRs in the reduction of energy demand for heating and cooling, as well as indoor air temperature, resulting in a decrease of energy consumption and an improvement of thermal comfort. The thermal behavior and energy efficiency of buildings are dependent on the characteristics of the building envelope. Consequently, GRs as part of the building envelop play a significant role in energy efficiency [90–92] and thermal comfort [56,93–100]. The energy performance of GRs depends on the type of GR (intensive, extensive, etc.), the type of vegetation, the climatic conditions, and the shape and characteristics of the building [14,25,101].

The reduction in outdoor temperature is proportional to the surface area of the GR and its vertical distance from the pedestrian level. The effect of the GR on the indoor thermal comfort depends on the reduction of the roof temperature and is confined to the floor where the green roof is installed. Regarding thermal comfort, the majority of publications discuss the reduction in indoor air or surface temperature.

Table 4 provides a summary of the most important quantitative findings pertaining to the reduction in energy consumption and the improvement of thermal comfort. The following may be highlighted from these findings:

(a) GRs contribute to a substantial decrease in the cooling load and an increase in annual energy savings.
(b) The cooling load was reduced by up to 70% was achieved, while annual energy savings ranged from 10 to 60%.
(c) GRs can reduce the indoor air temperature significantly. In several cases, this reduction was measured or projected to reach 15 °C.
(d) GRs with trees outperformed simple GRs, even when the latter had greater coverage.
(e) By shading a building with nearby trees, it was possible to reduce further the internal temperature.
(f) The combination of GR and green walls can achieve a greater reduction of indoor temperature and improve thermal comfort.

4. Environmental benefits

The environmental benefits of GR have been well documented by various researchers. In this section the key aspects of the environmental performance of GRs are analyzed. These include an improvement in air quality; a significant controlling effect on the runoff water volume and contribution to pluvial flood mitigation; an impact on indoor environmental quality; and a reduction in environmental noise.

Environmental benefits as presented in section 4 consist of air quality improvement (sub-section 4.1), and improving runoff water quality (sub-section 4.2). Moreover, air quality improvement (sub-section 4.1)

Table 2
Summary of the main constructional and operational characteristics, experimental period, location, measured parameters, and main results of experimental GR studies.

Reference	Construction and operational elements	Experimental period	Location	Measured parameters	Main results
[3]	Roof lawn garden. A planting layer made of non-woven fabric instead of soil, a drainage layer, and a root barrier layer. The lawn size was about 4 × 9 m, the thickness of the fabric layer was about 8 cm (including the drainage and root barrier layers), while the lawn thickness was 3 cm.	Summer 1991	Osaka, Japan	Outdoor air temperature and relative humidity, solar radiation, rainfall, and concrete slab surface temperature	Significant reduction of indoor temperature in the space underneath the roof lawn garden. The slab roof surface temperature decreased by 30 °C during the summer thus expecting a heat flux reduction of up to 50% entering the room (under the roof).
[77]	An extensive GR system covering the 40% of the total roof area was installed in a two-story nursery school building.	Three months (4/9/2002–12/12/2002)	Athens, Greece	Ambient air temperature, indoor air temperature values in the two building floors, and indoor and outdoor relative humidity	The GR system contributed to a significant reduction of cooling load during the summer, which ranged from 6 to 49% for the entire building, and from 12 to 87% for its last floor.
[78]	Two test cells were constructed: (a) A "concrete" test cell made of simple grey pavement, and (b) a "green" test cell with the planted roof.	5 days, August 2004	Cardiff, UK	Indoor and outdoor surface temperature and relative humidity	The external concrete surface temperature fluctuated between 14 and 38 °C; the internal concrete surface temperature varied from 16 to 38 °C; the external green surface temperature varied from 22 to 27 °C; and the internal green surface temperature fluctuated between 23 and 28 °C.
[79]	The canopy layer was about 7 cm in depth with 100% coverage ratio, while the LAI was equal to 4.6	11 days, July 2009	Guangzhou, South China	Global solar radiation, wind speed, ambient air temperature, dew point, soil and plant temperature, soil water content, and heat fluxes	(a) Theoretical values were in good agreement with experimental results. (b) When soil water content was high, solar radiation was responsible for 99.1% of the total heat gain, while convective fluxes represented only 0.9%. (c) Evapotranspiration was responsible for 58.4% of dissipated heat, longwave radiative exchange between the canopy and the ambient air for 30.9%, photosynthesis for 9.5%, while the rest 1.2% was stored by soil and vegetation or was transferred into the space beneath.
[80]	A GR consisted of a concrete slab, beams, a drainage layer, and a filter layer. The LAI was found equal to 2.	Cooling and heating periods (21–30 January 2013 for heating, and 5–11 July 2013 for cooling)	Lisbon, Portugal	Outdoor and indoor temperature and relative humidity, global solar radiation, surface temperature, and heat fluxes	Theoretical results were compared with experimental ones and the relative model was successfully validated
[40]	A GR system covered an area of 10,000 m^2 and hosted 16,000 indigenous aromatic plants of 14 different kinds. It was installed in a three-floor office building which was fully insulated.	Summer 2013	Athens, Greece	Indoor and outdoor air temperature, upper floor indoor roof surface temperature, surface temperature of the surroundings of the planted area, surface temperature of the plants and canopy area	GR system surface temperature was 15 °C lower than that of a conventional roof.
[45]	Measurements were performed in two experimental rooms, one equipped with a GR system and another covered with a common roof. The experimental GR system was an extensive green roof containing 36 prefabricated greenery modules. The soil substrate, about 4 cm in thickness, consisted of 60% peat soil, 10% powdered perlite, 20% vermiculite aggregate, and 10% organic fertilizer.	Summer 2014	Shanghai, China	Temperature values at different layers, indoor and outdoor temperature, wind speed, solar radiation, rainfall, relative humidity, heat fluxes, and volumetric content of soil moisture	Solar radiation was strongly correlated with the cooling effect of the GR system, which is higher during sunny days. Moreover, GR systems contributed to a reduction of the outer surface temperature amplitude variation by 32.5 °C, while the roof temperature difference between green and common roof increases was up to 5 °C.
[46]	An extensive roof covered an area of 5600 m^2. The soil substrate was based on minerals with 4–8% organic elements.	September 2013 to September 2015.	Syracuse, New York, USA	Air temperature, soil moisture, relative humidity, wind speed and direction, incoming solar radiation and rainfall-snowfall	Heat fluxes varied between −5.76 Wm^{-2} to 9.46 Wm^{-2}, with negative values during the summer and positive during the winter, when accumulated snow may act as extra insulation
[47]	Three house-like cubicles had identical dimensions with the following characteristics: the first had a conventional insulated flat roof, while the other two had extensive GRs 9 cm deep instead of	Heating and cooling period in 2012 and part of 2013	Puigverd de Lleida, Spain	indoor ambient air temperature and humidity, indoor wall temperatures, electrical consumption of heat pumps, total solar radiation, and outdoor air temperature and humidity	Experimental results showed a significant reduction of the energy consumption in the extensive GR cubicles compared with the reference one, reaching 16.7% during the summer. During the winter, the energy consumption in the two GR cubicles

(*continued on next page*)

Table 2 (*continued*)

Reference	Construction and operational elements	Experimental period	Location	Measured parameters	Main results
	an insulation layer. All cubicles were equipped with an HVAC system for heating/cooling purposes.				increased by 11.1% compared to the reference one.
[48]	Two identical house-like cells were constructed, with only the following difference: one cell was covered with a roof made of a bare concrete slab without insulation, while the other one was covered with an extensive GR above an insulation 15 cm thick, with a soil substrate thickness of 5 cm.	Cooling periods in 2015 and 2016	Chongqing, China	Outdoor and indoor air temperature, outdoor and indoor relative humidity, solar radiation, wind speed, concrete slab surface temperature, leaf temperature, soil temperature, roof heat fluxes, optical thermal properties in the canopy layer	Experimental results showed that a significant reduction of indoor air temperature and heat gain was obtained with the combination of a GR system with night ventilation. The combination of a GR and night ventilation led to a heat gain reduction of up to 79%.
[22]	Seven extensive GR systems, with the same dimensions, installed on the roof of a one-story school building. A part of the roof was covered by a conventional white gravel for comparison purposes. The GRs consisted of a 2 cm thickness drainage layer, a cloth layer of 0.3 cm, and a soil substrate layer with vegetation. The substrate layer with a root barrier was 3.5 cm thick while the vegetation was a mixture of stonecrop (sedum) species.	2010 to 2015	Utrecht, Netherlands	Outdoor air temperature, solar radiation, wind speed, and rainfall, air temperature above the ground at 15 and 30 cm at the center of each green roof, soil temperature 2 cm under each GR surface and under the gravel layer, soil moisture in the substrate layer and runoff	Compared with a conventional gravel roof, the ambient air above GRs was colder during the night and warmer during the day, thus displaying a beneficial cooling effect during the night when the UHI effect is stronger.
[23]	Four plots of a surface 50 m^2 each were constructed on a roof, leaving one plot with conventional roof surface as a "reference" plot for comparison. The other three plots were experimental extensive GR systems with small differences regarding vegetation, insulation layer thickness, and hydraulic properties of materials used.	2016 to 2017	Calabria, Italy	Ambient air temperature, total solar radiation, longwave radiation, relative humidity, wind speed and direction, rainfall, atmospheric pressure, soil substrate temperature, and volumetric water content	The annual energy savings for a non-insulated GR reached 34.9% in continuous, and 34.7% in intermittent operation, with the higher energy saving obtained in the summer

includes pollutants deposition (4.1.1), carbon sequestration (4.1.2), and indoor air quality (4.1.3).

4.1. Improvement of air quality

With their leaves, branches, and foliage, plants create an excellent air pollution sink [126,127]. Plant species possess the following significant abilities to reduce air pollution and limit emissions [128–131]: (a) they remove air pollutants (O_3, NO_2, SO_2) and capture particles and dust matter through leaf stomata with deposition processes [5,132,133]; (b) they can decrease surface temperature values by shading or natural cooling through evapotranspiration, thereby reducing photochemical reactions responsible for creating air pollutants, and contributing to energy savings for cooling thus reducing CO_2 emissions [129,130]; and (c) they play a key role in carbon sequestration through photosynthesis [134].

Although vegetation use as a filter for polluted urban air has been extensively studied and documented, the contribution of GRs to the reduction of air pollution has not been adequately addressed in the scientific literature.

4.1.1. Deposition of pollutants

The reduction of air pollution through the stomata of leaves has been researched and quantified using measurements and deposition models.

Yang et al. [132] quantified the reduction in air pollution effected by 170 extensive, semi-intensive, and intensive GRs in Chicago using a dry deposition model. The model was based on the calculation of leaf stomatal resistance, which is a function of photosynthetically active radiation, air temperature, leaf water potential, and vapor pressure deficit [135]. Nitrogen dioxide (NO_2), sulfur dioxide (SO_2), ozone (O_3), and particulate matter smaller than 10 μm (PM_{10}) were studied as pollutants. Different GR planting scenarios that account for the reduction of air pollution have supplemented research. It was determined that 19.8 ha of GRs cleared a total of 1675 kg of air pollutants over the course of one year, with 52% pertaining to O_3, 27% to NO_2, 14% to PM_{10}, and 7% to SO_2 concentrations.

In [51], an experimental investigation of the ability of four GR vegetation species to capture PM_{10} was presented and analyzed. Creeping bentgrass (Agrostis stolonifera), red fescue (Festuca rubra), ribwort plantain (Plantago lanceolata), and sedum (Sedum album) were the vegetation species. Two GRs were chosen for an experimental investigation in Manchester, UK. Plants were transplanted into the GRs, and the efficiency of vegetation species to filter particulate matter was compared. Species A. stolonifera and F. rubra were shown to be more efficient in capturing PM_{10} particles. Finally, a scenario was developed for the center of the city of Manchester, calculating the annual PM_{10} removal potential under the assumption that all flat roofs in a particular area were vegetated. This scenario was shown to allow for a PM_{10} removal of 0.21 tons.

Tong et al. [136] performed an experimental case study analysis of the vertical profile of particulate matter smaller than 2.5 μm ($PM_{2.5}$) along an elevation gradient at a vegetated rooftop farm in the US, 26 m above the ground, under different meteorological conditions. Experiments and observations showed a 7–33% reduction of $PM_{2.5}$ concentrations in comparison to curbside levels.

Gourdji [137] reviewed the impact of extensive and intensive GR vegetation species on the reduction of air pollution (especially PM, O_3, and NO_2), and gave specific recommendations for GR vegetation species for Montreal, Canada. It was concluded that intensive GRs are preferable for the removal of air pollutants; PM could be captured and removed

Table 3
Summary of results of parametric studies.

Reference	Parameters	Results
[58]	(a) LAI (b) Thickness of soil layer (c) Evapotranspiration	(a) An increase of LAI from 2 to 5 led to a strong reduction of the solar transmittance of the canopy. (b) The thermal diffusivity of the soil was affected by the soil layer's thickness, density, and moisture content. (c) Evapotranspiration influenced both the state of the hydrothermal canopy and the energy flow through the GR system.
[34]	LAI	An increase of the LAI from 0.5 to 3.5 could result in reducing the canopy fluctuation amplitude of the air temperature from 11.6 °C to 3.6 °C, thus reducing the energy demand by 4 W/m^2.
[61]	(a) LAI (b) Irrigation	(a) An increase in the LAI led to an improvement in the shading effect and a minimization in the cooling load, but had a negative effect during the winter. (b) Increased irrigation during the summer period had a slightly beneficial effect on energy savings.
[85]	(a) LAI (b) Roof insulation	(a) For the summer period, an increase of LAI resulted in a decrease of the cooling load. (b) When a GR system was installed on the uninsulated roof, a 48% reduction in heating demand was achieved.
[82]	(a) LAI (b) Soil thickness (c) Insulation thickness	(a) & (b) LAI and insulation thickness had the greatest impact on cooling energy savings. (c) A non-insulated GR system could be very energy efficient during the summer but less so in the winter.
[35]	(a) LAI (b) Soil layer thickness	(a) A LAI increase from 0.001 to 5 resulted in cooling energy savings from 6.30 GJ to 11.82 GJ, while the heating energy savings decreased from 6.16 GJ to 3.76 GJ. (b) An increase of soil thickness from 0.05 to 0.7 m resulted in an increase of the cooling energy saving from 8.28 GJ to 12.19 GJ, while the heating energy savings were also increased from 2 GJ to 5.96 GJ.
[36]	LAD	Simulations results showed that an increase of LAD led to a remarkable reduction of the cooling load.
[81]	(a) GR system parameters: foliage height and density, soil layer thickness, type of planted roof, and thickness of the insulation layer. (b) Climatic parameters: air relative humidity, and wind speed.	(a) The influence of foliage height was not found to be a significant system characteristic by itself, but in conjunction with vegetation density. The thickness of insulation layer can play an important role, as its increase results in a decrease of the cooling potential of the system. The thickness of the soil layer was not found to have a significant contribution to the cooling efficiency of the system. (b) The relative atmospheric humidity plays the most significant role, as it is strongly correlated with evapotranspiration. A wind speed increase resulted in reducing humidity, thereby enhancing evapotranspiration and the cooling capacity of the system.
[77]	Plant coverage	An increase of the plant coverage of a GR decreased its substrate surface temperature, resulting in a reduction of the cooling load. There was an increase in the heating load as plant coverage increased. However, this increase was much lower than the decrease of the cooling load.
[83]	Climatic parameters: incident solar radiation, evapotranspiration rate, ambient air temperature, and wind speed.	Linear correlations were found between the indoor air temperature and the incident solar radiation, and between the evapotranspiration rate and both the ambient air temperature and wind speed respectively.
[26]	Roof insulation	The greatest annual energy savings were achieved for a non-insulated building equipped with a GR system and amounted to 37%. For a moderately insulated building, the annual energy savings ranged from 4 to 7%, whereas for a well-insulated building the annual energy savings were less than 2%.
[30]	Roof insulation	During the summer, the reduction in cooling load due to the GR system varied between 15 and 49% for non-insulated, and between 6 and 33% for insulated buildings. The impact of GR on heating load was negligible.

more effectively by pines; O_3 could be removed more efficiently by drought tolerant, deciduous broadleaved trees; and small cold-tolerant magnolias were effective plants for the removal of NO_2. Taking into account the pollutant emissions in Montreal, it was determined that an 88% GR coverage with Pinus mugo var. pumilio (dwarf mountain pine) could remove 92.37 kg of PM_{10} annually (35.10 kg of which were $PM_{2.5}$).

Dry deposition modeling was used in Ref. [138] to evaluate the potential of GRs to reduce tropospheric O_3 concentrations and improve the outdoor air quality around a building. It was shown that the O_3 concentrations attained were reduced by 0.25–1.8 μg/m^3.

4.1.2. Carbon dioxide reduction and carbon sequestration

The reduction of atmospheric CO_2 by GRs could be achieved with two main processes: (a) through the natural process of photosynthesis, where carbon sequestration is obtained in plants and foliage; and (b) through evapotranspiration, which provides a significant reduction of the surface temperature, resulting in a decrease in energy demands, and mitigation of the urban heat island [133]. Selecting the appropriate plants species as well as the depth and composition of the substrate, can increase the amount of net carbon sequestered. Several studies in the scientific literature have demonstrated that vegetation type and soil

Table 4
Summary of the main implementation methods, investigation modes, and main energy efficiency results for GR studies.

Reference	Implementation method	Investigation mode	Experimental or theoretical calculations area	Energy efficiency results
[26]	Simulation and experimental	Cooling effect for experiment and entire year for theoretical calculations	Near Athens, Greece	(a) Energy savings of 37% for the entire year were calculated for a non-insulated building with GR, which reached 48% when night ventilation was also applied. (b) Indoor air temperature values for a typical summer day and for the building with GR were found to be significantly lower than those without the GR.
[27]	Simulation and experimental	Cooling effect for experiment and entire year for theoretical calculations	Singapore	(a) Energy savings of 17–79% were found in the cooling load and savings of 1–15% in the annual energy consumption. (b) Clay soil was found to be the optimum solution for energy conservation, achieving energy savings of 64% for space cooling, 71% for the peak space load, and 3% for the annual energy consumption. (c) The optimal type of vegetation was determined to be shrubs, which resulted in energy savings of 79% for space cooling and 15% for annual energy consumption.
[28]	Simulation and experimental	Cooling effect for theoretical calculations and the autumn period for experiment	Athens, Greece	(a) A cooling load reduction of 6–49% was found for the entire building, and 12–87% for the last floor. (b) An insignificant increase of heating load was observed.
[29]	Simulation	Cooling effect	Different climates: London, UK; Montreal, Canada; Moscow, Russia; Athens, Greece; Beijing, China; Honk-Kong; Mumbai, India; Brasilia, Brazil; Riyadh, Saudi Arabia	(a) The air temperature at the roof level decreased a to a maximum of 26 °C, and an average of 12.8 °C. (b) Green walls inside the urban canyon had a stronger cooling effect than GRs.
[30]	Simulation	Cooling effect	Athens, Greece	A remarkable 40% reduction of the cooling load was achieved.
[32]	ANN model and experimental	Cooling effect	Sustainable city, Ujjain, India	A GR system was effective in reducing the indoor air temperature and energy consumption during the summer. The mean indoor air temperature did not exceed 28 °C, while the cooling potential of a GR in a typical summer day in India was 1.25 kW.
[33]	Simulation	Cooling effect	European climates: Crete, Greece; Rome, Italy; London, UK	Green and cool roofs proved to be excellent technologies for the mitigation of the urban heat island effect and could contribute significantly to both the amelioration of the urban climate and the reduction of building energy demands.
[36]	Simulations and experimental	Cooling effect	Continental Mediterranean climate	(a) The GR cooling effect was strongly depended on LAD. (b) An indoor air temperature reduction up to 2 °C was found when there were trees nearby the examined building apart from the GR.
[78]	Experimental	Cooling and heating effect	Athens, Greece	(a) A GR can function satisfactorily as an insulation layer. (b) The surface temperature values of planted area were significantly lower than those of the conventional roof, contributing to the reduction of global warming. (c) The overall annual energy reduction during the cold and hot periods was found to be significant, reaching 15.%, with the reduction of the cooling load reaching 18.7% and of the heating load reaching 11.4%.
[79]	Simulation	Cooling effect	Tropical climate, Singapore	On a summer day, GR can reduce heat gain by 13.14 kWh/m^2 (31%).
[80]	Experimental	Cooling effect	Utrecht, Netherlands	A sedum-covered GR offers a slight warming effect at daytime and a significant cooling effect at nighttime, contributing to the mitigation of nocturnal urban heat island.
[59]	Simulation	Cooling and heating effect	Warm and cold European climates	(a) In warm climates, GRs can contribute to a reduction of the cooling load without a significant increase of the heating load, offering an annual energy demand reduction up to 11%. (b) For cold climates, GRs offered a decrease in both heating and cooling energy demand, contributing to energy savings up to 7%.
[66]	Simulation	Cooling effect	–	Compared to a building with a conventional roof, a building with a GR system exhibited a significant

(*continued on next page*)

Table 4 (*continued*)

Reference	Implementation method	Investigation mode	Experimental or theoretical calculations area	Energy efficiency results
				decrease in indoor air temperature., leading to a remarkable reduction of the cooling load.
[67]	Simulation and case study	Cooling and heating effect	Three different climates of Iran	(a) GR systems contribute to a decrease of energy consumption for cooling and heating, which could be greater for higher LAI values. (b) An increase of the soil layer thickness resulted in an increase of cooling and a decrease of heating energy consumption. (c) The combination of a GR with fewer building floors could be more effective for energy savings.
[85]	Simulations and testing in three cities with different climates, (Athens, La Rochelle, and Stockholm)	Cooling and heating effect	La Rochelle, France	(a) It was observed that GR systems had a remarkable 52% impact on cooling demand. (b) A GR system did not have a significant impact on heating demand. (c) A reduction of the total annual energy demand was observed, amounting to 32% for Athens, 6% for La Rochelle, and 8% for the cold climate of Stockholm.
[102]	Simulation and Experimental	Cooling effect	Osaka, Japan	(a) A decrease of GR slab surface temperature from 60 to 30 °C was observed. (b) A 50% reduction of heat fluxes into the room underneath was also observed.
[103]	Simulation and experimental	Cooling and heating effect	Lisbon, Portugal	(a) The energy performance of three GR types was investigated: extensive, intensive, and semi-intensive. (b) As regards heating requirements, the three types presented a similar energy efficiency behavior. In terms of cooling requirements, semi-intensive and intensive green roofs required 36 and 17% less energy than extensive green roofs, respectively.
[104]	Simulation and experimental	Cooling and heating effect	Athens, Greece	(a) The surface temperature difference between a green and a conventional roof was measured to be up to 15 °C. (b) Indoor air temperature values during the summer decreased by up to 0.8 °C. (c) A significant reduction of the annual energy consumption was calculated, which was up to 19% for the cooling and up to 11% for the heating load.
[105]	Field experiment	Cooling and heating effect	Shanghai, China	(a) A GR presented a remarkable cooling effect during the summer period, with a maximum heat flux difference between the GR and a conventional roof up to 25 W/m^2. (b) A GR contributed to a reduction of the amplitude fluctuations of the outer surface temperature by 23.5 °C.
[106]	Simulation and experimental	Cooling and heating effect	Syracuse, New York, USA	Heat fluxes varied between −5.76 Wm^{-2} to 9.46 Wm^{-2} with negative values during the summer and positive during the winter, when accumulated snow acts as an extra insulation layer.
[107]	Experimental	Cooling and heating effect	Spain	Experimental results showed a significant reduction of the energy consumption in the extensive GRs compared to the conventional one, reaching 16.7% during the summer. During the winter, the energy consumption in the GR increased by 11.1% compared to the conventional one.
[108]	Simulation and experimental	Cooling effect	Three different climates of China	A combination of a GR with night ventilation could achieve a reduction of the heating gain of 75–79%.
[109]	Simulation and experimental	Cooling and heating effect	Calabria, Italy	The annual energy savings for a non-insulated green roof were 34.9% in continuous and 34.7% in intermittent operation, with the highest energy savings obtained in the summer.
[110]	Simulation and case study	Cooling and heating effect	Republic of Korea	(a) A GR reduced the annual energy demand by a maximum of 90.9 GJ (3.7%). (b) A GR contributed to a significant reduction of the cooling load and a smaller reduction of the heating load.
[111]	Simulation	Cooling and heating effect	Chinese climates	(a) If applied to non-insulated roofs, a GR can contribute to a significant reduction of the cooling and the heating loads. (b) If the GR system was installed on a roof that was already insulated, the reduction in heating and cooling loads was minimal.

(*continued on next page*)

Table 4 (*continued*)

Reference	Implementation method	Investigation mode	Experimental or theoretical calculations area	Energy efficiency results
[112]	Simulation and experimental	Cooling and heating effect	Near Athens, Greece	(a) High energy savings were achieved for heating (21.4–21.8%) when compared to a non-insulated roof. (b) Energy savings for heating were drastically reduced when a GR was applied to a well-insulated roof. (c) Significant cooling energy savings ranging from 60.5 to 62.5% were obtained, compared to a non-insulated roof. (d) All examined GR systems presented high energy savings for cooling, compared to well insulated roofs, because of the evapotranspiration cooling effect.
[113]	Simulation	Cooling and heating effect	Amman, Jordan	Green roofs in their simplest applications could offer an annual energy saving of up to 17%, which could be increased if more complicated and advanced GR systems are used.
[114]	Simulation and case study	Cooling and heating effects	London, UK	(a) GR systems could reduce heating and cooling load. However, the energy reduction for cooling depends strongly on the irrigation status. (b) Regarding the reduction of the cooling load, GRs, are more effective at nighttime.
[115]	Simulation and experimental	Cooling effect	Chicago, USA	The daytime roof temperature decreased with increasing GR coverage, from less than 1 °C for 25% to 3 °C for 100% green roof.
[116]	Simulation and case study	Cooling and heating effect	Toronto, Canada	(a) The average reduction in indoor air temperature for the entire building was calculated to be 0.4 for an LAI of 1 and 0.7 for an LAI of 2. (b) The reduction of the total energy consumption varied from 1.8 to 2.9% for an LAI equal to 2 and a soil depth of 30 cm.
[117]	Simulation and experimental	Cooling and heating effect	Shanghai, China	(a) The energy savings of a GR system combined with ventilation reached 26.7%. (b) The indoor air temperature for a building equipped with GR combined with intermittent ventilation was kept below 29 °C for the air-conditioning season.
[118]	Simulation	Cooling effect	Four different climates: Hong Kong, Paris, Cairo, and Tokyo	A cooling load reduction of 5.2% was observed for the hottest day of the year in the hot-dry climate and with the full intensive GR system, while energy savings of at least 0.1% were found for a temperate climate and semi-extensive GRs.
[119]	Simulation and experimental	Cooling and heating effect	Shanghai, China	(a) Compared to a common roof during the summer, a GR presented an average cooling effect of 2.9 °C on the outer deck surface. (b) A GR could reduce the cooling and heating energy needs at the top floor up to 3.6% and 6.2% respectively. (c) During the winter, a GR can act as effective insulation.
[120]	Simulation	Cooling effect	Mexico City	A GR presented a significant cooling effect during the summer, reducing indoor temperature values by up to 12 °C.
[121]	Simulation and experimental	Cooling and heating effect	Eight cities in Mexico	(a) A GR could reduce the indoor air temperature by up to 4.7 °C in locations with a warm climate. (b) A GR could reduce the cooling energy demands by 99% in locations with a temperate climate, simultaneously increasing the heating demand by up to 25%.
[122]	Experimental	Cold and warm periods	Sub-arctic climate, Sweden	In a subarctic climate and for a fully insulated building, the energy benefits of a GR system are relatively low.
[123]	Experimental	Cooling effect	Nanjing, China (sub-tropical climate)	(a) A slight warming effect during the daytime, especially midday, was found. (b) A significant nighttime cooling effect was identified (c) The most remarkable cooling effect occurred at a height of 60 cm.
[124]	Simulation and case study	Cooling effect	Arid climates (Cairo)	(a) Extensive and intensive GR systems could contribute to a reduction of the cooling energy demand. (b) Compared to extensive GRs, intensive GRs were characterized by greater energy savings and temperature reduction.

(*continued on next page*)

Table 4 (*continued*)

Reference	Implementation method	Investigation mode	Experimental or theoretical calculations area	Energy efficiency results
[56]	Simulation	Cooling effect	Subtropical climates (Brisbane, Australia)	(a) The effect of the a GR on reducing the temperature was greater inside a buildings than outside, and the use of GRs with trees could reduce the indoor temperature by up to 7.2 °C, and air-conditioning electric load by up to 60%. (b) The performance of a GR with trees was superior to that of a simple roof, even if the latter had greater coverage.
[93]	Experimental (combination of a GR and a radiant/evaporative system)	Cooling effect	Los Angeles, USA	Even when the outside temperature was above 40 °C, the system was able to achieve indoor temperatures that were 9–13 °C cooler than those outside.
[94]	Simulation (shading in the building also provided by neighboring trees)	Cooling effect	Porto Alegre, Brazil	(a) A comparison of the indoor temperature of a building with and without a GR in a treeless environment revealed a difference of 2.8 °C during the summer months. (b) This difference increased by up to 4.3 °C when trees were present.
[95]	Experimental (combination of GR and green walls)	Cooling effect	Xiangtan, China	The maximum difference in operational temperature was 2.1 °C, and this difference was greater during the day.
[96]	Simulation	Cooling effect	Seoul, South Korea	An improvement in thermal comfort by 0.18–2.18% (using the PPD index) was noted.
[97]	Simulation	Cooling effect	Esch-sur-Alzette, Luxembourg; Palermo, Italy	It was estimated that the decrease in ceiling temperature by 2 °C in Esch-sur-Alsace and 5 °C in Palermo led to an improvement in the Predicted Mean Vote (PMV) index (from values greater than 0.5 to values less than 0.5).
[98]	Experimental and simulation	Cooling effect	Rome, Italy	During a typical summer week (from August 10 until August 17), the PMV index remained within the −1 to 1 range.
[99]	Measurement and simulation	Cooling effect	Dhaka, Bangladesh, (tropical climate)	Applying a GR to an industrial plant could reduce the indoor temperature by 2.5–3.5 °C.
[100]	Simulation	Cooling effect	Palermo, Italy	On the top floor, the effect of the GR was found to be significant, with the interior air temperature decreasing by a maximum of approximately 3 °C when both apartment doors and windows were open.
[125]	Experimental and simulation	Heating and cooling effect	Subtropical monsoon climate: Nanning, China	Eight GRs were experimentally tested in commercial and residential buildings. A reduction of the annual energy consumption ranging from 30 to 55% was demonstrated for various soil thicknesses.

substrate properties are the most influential factors on the overall performance of a GR in terms of carbon sequestration and pollutant concentration reduction [133,134,139,140].

Getter et al. [134] quantified carbon sequestration for an extensive GR in the US over a two-year period. The entire GR, including plants and soil substrate, stored 1188 gC/m^2, while the net carbon sequestration amounted to 378 gC/m^2, given that the original substrate contained 810 gC/m^2.

In [39], a comprehensive investigation of the effect of plant selection of a GR on carbon sequestration was presented. The analysis revealed that Sedum acre, Frankenia thymifolia, and Vinca major are capable of contributing significantly energy conservation and carbon sequestration. The use of these three plants reduced the annual energy consumption of a typical building by 8.5, 8, and 7.1% respectively, while the annual CO_2 absorbed by photosynthesis was 0.14, 2.07, and 0.61 kg/m^2 respectively. In addition, the relative reduction in annual CO_2 emissions caused by evapotranspiration for these three plants was calculated to be 28.16, 26.48, and 23.44 kg/m^2.

A three-part investigation was presented in Ref. [141], including (a) field measurements of the CO_2 concentrations in a GR in the subtropical climate of Hong Kong, (b) CO_2 absorption velocity and emissions rate of plants in a sealed glass chamber, and (c) theoretical calculations of the profile of CO_2 concentrations around a GR. For a typical sunny summer day, the CO_2 absorption was shown to be much higher during the day, probably because the photosynthetic process is strongly depended on the visible part of the solar spectrum. Moreover, CO_2 absorption depends on the species and condition of plants, the position of the GR, and the ambient airflow. It was found that, on a sunny day, the vegetated roof could reduce CO_2 in the surrounding area by almost 2%.

In [142], the annual surface-atmosphere exchange of CO_2 above an extensive GR in Berlin, Germany, was measured using the Eddy covariance technique. The results showed that the GR acted successfully as a carbon sink at a rate of 85 gC/m^2. The authors concluded that water availability, appropriate vegetation, and soil substrate could maximize carbon sequestration.

In Chengdu, China, Luo et al. [143] studied the carbon sequestration of a GR with six segments, two types of soil substrates, three substrate depths (20, 25, and 30 cm), and three different native vegetation species (Ligustrum vicaryi, Neottia auriculata, and Liriope spicata) over the course of a year. The average carbon sequestration was determined to be 6.47 kgC/(m^2·yr). The best carbon sequestration configuration was that of L. vicaryi, reaching 7.03 kgC/(m^2·yr).

In [144], the carbon sink potential of a GR in Japan was evaluated for three different grass species and soil substrates. The results showed that the annual CO_2 reduction due to energy savings varied from 1703 to 1889 kgCO_2/(m^2·yr). Biomass ash raw material coupled with wheat straw and sludge as a GR substrate, may be used for the manufacture of CO_2 solid adsorbents for CO_2 capture as well as for CO_2 absorption directly [145].

Table 5 provides a quantitative summary of the findings of research studies on the benefits of GRs in reducing air pollution. The analysis of the literature organized in Table 5 shows clearly the combined effect of GR systems in tackling various environmental challenges, such as improving urban air quality by significantly reducing pollutant

Table 5
Summary of the cited research studies regarding the reduction of air pollutants by GRs.

Reference	Methodology	Location	Pollutant	Results
[132]	A dry deposition model was used for 170 extensive, semi-intensive, and intensive GRs.	Chicago, USA	NO_2, SO_2, O_3, PM_{10}	1675 kg of air pollutants were removed by 19.8 ha of GRs in one year with 52% pertaining toO_3, 27% to NO_2, 14% to PM_{10}, and 7% to SO_2.
[51]	An experimental investigation aiming at comparing four GR vegetation species as regards their ability to capture PM_{10} (Agrostis stolonifera, Festuca rubra, Plantago lanceolata, and Sedum album).	Manchester, UK	Particulate matter (PM_{10})	(a) A. stolonifera and F. rubra were more efficient in capturing PM_{10} particles. (b) A scenario calculating the annual PM_{10} removal potential was developed for the center of Manchester, considering that all flat roofs in a selected area were vegetated. According to this scenario, a PM_{10} removal equal to 0.21 tons was achieved.
[136]	An experimental investigation of the $PM_{2.5}$ vertical profile along an elevation gradient at a vegetated rooftop farm in the US, 26 m above the ground under different meteorological conditions.	Brooklyn Grange, USA	Particulate matter ($PM_{2.5}$)	Experiments and observations showed a 7–33% reduction of $PM_{2.5}$ concentrations compared to curbside concentrations levels.
[137]	Authors reviewed the impact of extensive and intensive GR vegetation species on the reduction of air pollution.	Montreal, Canada	NO_2, O_3, PM_{10}, and $PM_{2.5}$	Intensive GRs is preferred for air pollutants removal. PM could be more effectively removed by pines; O_3 by drought tolerant, deciduous broadleaved trees; and NO_2 by small cold-tolerant magnolias. Calculations showed that an 88% GR coverage with Pinus mugho var. pumilio can remove 92.37 kg of PM annually (35.10 of which is PM2.5).
[138]	Field measurements and dry deposition modeling.	Portland, USA	O_3	Achieved O_3 concentration reduction varied from 0.25 to 1.8 μgr/m^3.
[134]	Experimental quantification of carbon sequestration provided by an extensive GR.	USA	Carbon sequestration	The entire GR, including plants and soil substrate, stored 1188 gC/m^2, while the net carbon sequestration was found equal to 378 gC/m^2, taking into account that 810 gC/m^2 existed in the original substrate.
[39]	An experimental investigation of the impact of GR plants on carbon sequestration	Mashhad, Iran	Carbon sequestration	*Sedum acre, Frankenia thymifolia*, and *Vinca major* could provide an excellent contribution to carbon sequestration. The use of these three plants offered an annual energy consumption decrease for a typical building reaching 8.5, 8, and 7.1% respectively, while the annual CO_2 absorbed by these three plants through photosynthesis equalled 0.14, 2.07, and 0.61 kg/m^2 respectively. The relative reduction of the annual CO_2 emissions caused by the evapotranspiration provided by the three plants, was 28.16, 26.48, and 23.44 kg/m^2 respectively.
[141]	Field measurements in a green roof in the sub-tropical climate of Hong Kong, of plants' CO_2 absorption velocity and emissions rate in a sealed glass chamber, and theoretical calculations of CO_2 concentrations profile around a green roof.	Hong Kong	Carbon sequestration	a) For a typical sunny summer, the CO_2 absorption was much higher during the daytime, because of photosynthesis. b) The absorption of CO_2 depended on plant species and condition, the GR position, and ambient airflow. c) For a sunny day, the vegetated roof was able to reduce CO_2 in the surrounding area by almost 2%.
[142]	The Eddy covariance technique was used for measuring the annual surface-atmosphere exchange of CO_2 above an extensive GR.	Berlin, Germany	Carbon sequestration	The GR succeeded in playing the role of a carbon sink with a rate of 85 gC/m^2, while the authors concluded that water availability, appropriate vegetation, and soil substrate could optimize carbon sequestration.
[143]	A GR consisted of six segments with two kind of soil substrates, three substrate depths, (20, 25, and 30 cm), and three vegetation species.	Chengdu, China	Carbon sequestration	The average carbon sequestration equaled 6.47 kgC/m^2·yr. The best carbon sequestration configuration was that of L. vicaryi and was equal to 7.03 kgC/m^2·yr.
[144]	The sink potential of a GR in Japan for carbon sequestrating was measured for three different grass species and different soil substrates.	Japan	Carbon sequestration	Annual CO_2 decrease caused by energy savings varied from 1703 to 1889 kgCO_2/m^2·yr.

concentrations (e.g. $PM_{2.5}$, PM_{10}, O_3, NO_2) and sequestering carbon, thereby making a substantial contribution to climate neutrality.

4.1.3. Indoor environmental quality

GRs have a positive impact on indoor and outdoor thermal comfort. Concerning outdoor comfort, this refers to the reduction of surface and ambient temperature, particularly during the summer, along with a reduction in the cooling load. Various studies have investigated indoor and outdoor comfort conditions [146–150]. GRs can also have a positive impact on the indoor temperature, as demonstrated by Ref. [151], which compared indoor temperature measurements of a single story building in Malaysia equipped with a white and a green roof. Similar conclusions were drawn in Ref. [26], through experimental and simulation analyses during the summer in Greece.

The interaction of GRs with indoor air, as particles from the substrate and vegetation are suspended and entrained in the local rooftop air flow, has not been studied extensively. In Ref. [152], a load of HVAC filters was examined on the roof of a big-box retail store in Portland, US. Results revealed the potential for increased concentrations of volatile organic carbon compounds (VOCs), especially methanol; however, the authors noted that it was difficult to detect trends of VOC fluxes or other selected compounds, due to temperature, relative humidity (RH), or seasonality. In Ref. [138], the impact of green roof-O_3 interactions near the exterior ventilation air supply of a building was evaluated for the roof mentioned previously; the effect of GRs on reducing rooftop-scale O_3 levels was moderate.

4.2. Improving runoff water quality

Numerous research studies have examined the ability of GRs to retain urban rainfall runoff [5,20,40,133,153–158]. Stormwater retention, which typically ranges between 40 and 60% of total rainfall, depends on several factors, such as GR type, substrate depth, composition and humidity, vegetation species, plant size, as well as rainfall duration and intensity [159,160].

Although the ability of GRs to manage the quantity of urban runoff has been well documented in the scientific literature, the impact of GRs on the water quality of runoff has been inadequately defined and

remains ambiguous. The fundamental argument relates to how a GR impacts the quality of runoff water, i.e. how it affects pollutants and effluents, and whether it acts as a sink or a source of pollution.

Table 6 summarizes the findings of several research studies regarding the effect of GRs on runoff water pollution, focusing on how a GR system impacts water pollution.

5. Noise reduction

A GR on a building contributes to noise reduction in both the urban environment outside the building as well as the living, working, or recreational environment inside the building. The former is attributed to the increased sound absorption characteristics of a GR compared to a standard (non-vegetated) roof, while the latter to the increased transmission loss provided by a vegetated roof compared to a standard roof. The increased transmission loss is discussed in section 5.1 and the effect of increased sound absorption in sections 5.2 and 5.3.

Sound reaches the roof of a building from a multitude of sources, such as air-traffic (particularly for houses close to airports or heliports and/or directly below the flight paths), elevated ground-transportation, ground-traffic (reaching the edge of the roof either directly or after reflection on the facades of higher buildings), and sound trapped in urban canyons.

5.1. Indoors sound - transmission

Part of the sound energy that eventually reaches the roof of a building is transmitted through the multiple layers of a GR. The transmission loss, T_L, or the sound reduction index, R, computed or measured for each frequency, show the sound energy lost during transmission at the specific frequency. The range of frequencies typically considered for indoor sound is 125−4000 Hz. The overall weighted sound reduction index, $R_{W,}$ is a single number over all frequencies. High T_L, R, or R_w values, all measured in dB, indicate improved sound insulation and a quieter environment inside the building.

5.1.1. Models

Based on the lumped-element approach and the theory of sound transmitted through a thin Euler-Bernoulli plate, the spectrum of transmission loss may be separated roughly in three parts. The first part (starting from lower frequencies) is controlled by the stiffness of the plate, the second by its mass, and the third by its damping. Between the first and second part, there is an area of resonance yielding low transmission losses. Inside this latest part of the spectrum, the mass loading and the bending stiffness of the plate create the effect of coincidence, which is characterized by very small transmission losses around a frequency (the critical frequency of coincidence). A GR adds mass and damping to the system without changing its stiffness considerably. As a result, a GR should increase the transmission loss in the mass controlled area, weaken the coincidence effect, and/or move the critical frequency of coincidence outside the frequency range of interest.

5.1.2. Experimental evidence

Published experimental data are scarce and they regard only lightweight extensive GRs. Nevertheless, they clearly verify the above stated hypothesis. Connelly and Hodgson [164] showed that lightweight extensive vegetated roofs may increase transmission loss by up to 10 dB at low frequencies and up to 20 dB at mid-range frequencies. The noise reduction at low frequencies is important, as it cannot be achieved easily by other means (for example, by adding a ceiling underneath the roof).

Based on small sample experiments, Galbrun and Scerri [165] showed that the overall weighted sound reduction index achieved by GRs, R_w, is comparable to those of standard roofs. Specifically, a GR on plywood panel has a weighted sound reduction index comparable to a standard pitched roof with tiles on felt (R_w from 43 to 47 dB). Additionally, a GR with an 80 mm cavity underneath should achieve a sound

Table 6
Summary of cited research studies regarding the runoff water pollutant reduction effects by GRs.

Reference	Location	GR Type	Main Results
[161]	Connecticut, USA	248 m^2 extensive GR	(a) The GR acted as a sink for NH_3–N, Zn, and Pb, but also as a source for Cu, NO_3+ and NO_2–N, TP, PO_4–P, Hg, and Zn. (b) The GR increased the pH values of runoff water to 7 or 8, thus neutralizing the effects of acid-rain.
[40]	Japan and Sweden	Intensive GR in Japan and extensive GR in Sweden	(a) Both GRs acted as a sink for nitrate and ammonium nitrogen (NO_3–N, and NH_4–N). (b) Both GRs acted as a source for organic carbon and potassium. (c) Only the extensive GR contributed to phosphorous release. (d) An increase of the pH of runoff water was observed, thus neutralizing the effects of acid rain.
[50]	India	Pilot-scale GR, with different soil substrates, and four different system configurations, including planted and unplanted systems, and various artificial rain conditions	(a) GRs acted as contaminant sink for several metals, such as Ca, Mg, Al, Fe, Cr, Cu, Ni, Zn, Pb, Cd. (b) GRs increased the pH of acidic rain. (c) Soil substrate and vegetation choices were an additive factor influencing water quality.
[162]	Chongqing, China	Pilot-scale GR	(a) A satisfactory level of retention was achieved, ranging from 35.5 to 100%, with an average of 77.2%. (b) A neutralization of the pH of rainwater was achieved. (c) The GR acted as a sink for NH_4 +-N and as a source for NO_3–N, K+, Si_4+, Ca_2+, TOC (Total Organic Carbon), and DAI (Dissolved Al (Alouminium)).
[156]	Beijing, China	9 types of extensive GRs, with different soil substrates and depths, vegetation types, planting time and rainfall characteristics	(a) GRs contributed to the reduction of the concentration of some nutrients. (b) GRs increased the concentration of total nitrogen, ammonia nitrogen (NH_4+−N), and nitrate nitrogen (NO_3–N).
[163]	Dingxi, Gansu Province, China	Extensive green roof	(a) The extensive GR acted as a source for the majority of pollutants in the stormwater runoff. (b) The substrate material effect was

(continued on next page)

Table 6 (*continued*)

Reference	Location	GR Type	Main Results
			quite high on pH, electrical conductivity (EC), F−, NO_3−, and NO_2–N concentrations. (c) The vegetation type influenced the concentration of Cl−, SO_4^{2-}, and total phosphorus (TP).

reduction index comparable to a 100 m concrete roof (R_w equal to 50 dB). In that regard, green roofs may be seen as a replacement or as a re-enforcement of existing roofs.

5.1.3. Parameters

Both studies mentioned in the previous section [164,165] showed that the depth of the substrate (and the corresponding mass it adds to the system) is one of the primary parameters affecting the noise insulation offered by a GR. The moisture or the compaction of the substrate did not seem to play a role. Indeed, Galbrun and Scerri [165] provided an empirical curve to predict the transmission loss as a function of surface density.

Several other design parameters of the GR have also been tested and seem to require further investigation. For example, Connelly and Hodgson [164] noticed the effect of the different plant roots to the overall sound insulation. Galbrun and Scerri [165] investigated the effect of different drainage systems (membrane, gravel, and pebbles). A particularly interesting experimental finding was that adding a cavity to the system increased the overall weighted sound reduction index by 13 dB.

5.2. Outdoors sound - absorption

A green roof is a sound absorbing surface. Only part of the sound energy that reaches the roof is redirected back into the urban environment. The sound absorption coefficient, a, expressed as a percentage or as a fraction between 0 (no sound absorption) and 1 (complete sound absorption), characterizes the amount of sound that is absorbed by the GR. The higher the value of a, the quieter the urban environment. The sound absorption coefficient is measured (or computed) either for normal incidence (sound arriving normal to the roof) or for random incidence (sound arriving to the roof from random directions). The former is measured by the impedance tube method, while the latter by means of reverberation room measurements or, alternatively, by analysis of the normal incidence values [166]. In general, sound absorption increases with frequency and layer thickness. The typical range of frequencies for the applications at hand is 125 to 4000 Hz.

5.2.1. Experimental evidence

Published measured data substantiate the good acoustic performance of GRs as sound absorbing surfaces: Horoshenkov et al. [167] measured very high values of the normal incident absorption coefficient for winter Primula vulgaris atop (but not planted) a low density substratum (above 0.8 for all frequencies above 200 Hz). Yang et al. [168] reported that a layer of topsoil (i.e. the naturally occurring uppermost layer of soil that is relatively high in organic matter and nutrients) with 100% plant coverage reaches almost complete absorption at 1000 Hz for random incidence. Measurements for two types of commercial GRs (alveolar and hexa) showed high absorption coefficient (a equal to 0.7) for medium and high frequency and low absorption (a equal to 0.2) for low frequencies [169].

Pittaluga et al. [170] reported the values of the normal incidence sound absorption coefficient to be 0.5 at about 500 Hz for extensive GR samples, 0.85 at 450 Hz for semi-intensive, and 0.4 for common soil. For comparison, the absorption coefficient of a concrete roof is almost equal to zero. Connelly and Hodgson [171] reported that the random incidence absorption coefficient for the various vegetated roof plots that were tested was 0.2–0.3 at low frequencies and 0.5−0.6 at 1000 Hz. The noise reduction coefficient, NRC, of seventeen different vegetated roof plots that were tested ranged from 0.20 to 0.63. For comparison, the NRC of an exposed roof is 0.06. The NRC is the average of the sound absorption coefficients in the 250, 500, 1,000, and 2000 Hz octave bands.

5.2.2. Models

The mechanisms of sound absorption are not entirely understood. Possible mechanisms include the ground effect, the thermoviscous absorption in the soil and the boundary layer of air at the surface of the leaves, scattering from stems and leaves, and stem and leaf vibration. GRs are composed of a porous substrate and a plant layer. The two layers are modeled separately and very few models exist for their combined effect.

Specifically, the substratum is treated as a porous material described by various parameters. The model of Zwikker and Kosten [172] employed three parameters: porosity (volume fraction of air), flow resistivity of the porous material, and a structure constant (accounting for the specific structure of the pores and the frame of the material). The model of Attenborough [173] was based on porosity, flow resistivity, grain shape factor, pore shape factor ratio, and tortuosity (accounting for the total deviation of pore axes from a normal to the surface). The empirical model by Delany and Bazley [174] and Chessel [175], later adjusted by Miki [176], required only the flow resistivity. Recently, Connelly and Hodgson [171] presented a regression model with the parameters volumetric water content at wilting and field capacity, compaction, percentage of organic matter, and porosity.

The models for sound absorption by plants are noticeably fewer. Watanabe and Yamada [177] investigated sound propagation through vegetation (which is applicable in the case of sound propagation at near-grazing incidence through a GR). They considered the leaf as a flat plate and yielded a model for sound absorption, which was found to be proportional to the square root of the frequency and a constant. The larger the leaf area, the higher the sound absorption. Horoshenkov et al. [167] showed that the effective tortuosity of a plant is theoretically related to the dominant angle of leaf orientation. They also presented two empirical expressions to predict the effective flow resistivity (and thus the sound absorption) based on leaf area density, for small and large dominant angles of leaf orientation. The larger the leaf area density and the larger the dominant angle of leaf orientation, the higher the values of the acoustic absorption coefficient.

The combination of soil and plant layer is even more complex to model. In order to predict the absorption coefficient of a leaf in front of the surface of a porous substrate, Ding et al. [178] employed the equations from Biot's elastic frame porous medium model [179,180] and the isotropic plate vibration theory, and solved them using a finite-difference time-domain approach. Horoshenkov [181] modeled both the soil and the plant layer by employing the Miki empirical model [176]. The acoustical absorption of the plant-soil system was determined using a transfer matrix approach. In both cases, the plants/leaves were considered to lay on top of the soil. The effect of the roots growing into the soil was not modeled.

5.2.3. Parameters

Parameters that affect the sound absorption of GRs are: moisture; compaction; organic matter in the substrate; plant coverage; leaf area; leaf density and orientation; leaves on the ground; and plant development. The sound absorption of the bare substratum increases inversely to its moisture [171,181], increases with its depth [171,178], increases with the percentage of organic matter in the substratum [171], and

decreases with compaction [171]. The moisture contained in the substratum seemed to be the most important parameter. Conelly [171] reported considerable differences in sound absorption when testing oven-dried soil, soil in the wilting stage, and soil at field capacity. Horoshenkov et al. [182] reported that the difference in the absorption coefficient between moderately dry and heavily wetted soil specimens can be 5 to 10 times greater. Yang et al. [168] reported a slight increase with substratum depth, while Connelly [171] reported a more noticeable increase, both for random incidence. Several soil types including sand, compost, pumice, and various mixes have been tested, and the effect of the percentage of organic matter in the substratum seem to be of interest [171].

Leaves on top of a substratum increase sound absorption. A leaf on top of a porous substrate increases the absorption coefficient in the middle frequencies and decreases it at high frequencies [178]. The influence of a leaf becomes more pronounced when the leaf is added to a low-permeability substrate. A large pack of leaves on a porous substrate was measured to increase the absorption coefficient at all frequencies [183].

The absorption coefficient of vegetation increases with leaf size [168], and seems to be controlled by leaf area density and the angle of leaf orientation [167]. Connelly and Hodgson [171] reported that the absorption coefficient of GRs decreases as plant establishment progresses. Finally, a variability of the acoustic properties of GRs with time is expected, as the water saturation changes, plants develop, and the substrate gets compacted.

5.2.4. Variability and engineering

Published measurement data on the sound absorption of GRs and their elements show a considerable variability with regard to sound absorption. The various parameters of the samples tested as well as their combination seem to affect the acoustic performance of a GR significantly. This variability allows one to consider the possibility of engineering a GR in order to achieve specific noise reduction goals.

5.3. Outdoors sound - diffraction

Diffraction is the mechanism by which sound penetrates into an acoustical shadow zone. Consider a building situated between a noise source (such as road traffic) and a receiver (a person in the backyard of the building). The receiver is located in an acoustical shadow zone, as the direct sound from the road is blocked by the building. However, sound reaches the receiver, propagating as follows: (i) starting from the road, it diffracts on the upper edge of the building facing the road, (ii) it propagates at grazing incidence over the top surface of the building, and (iii) it diffracts again on the upper edge of the building facing the backyard, eventually reaching the receiver in the backyard. This is a case of double diffraction, as sound diffracts on two edges to reach the receiver. In other configurations, such as a higher building behind the one that faces the road, sound reaches the receiver directly after it diffracts on the first edge (single diffraction).

The exposed facade of the building and the roof form a right-angled wedge. So do the roof and the backyard facade of the building. For diffraction on wedges, the following are known. In general, the diffraction contributions are much smaller than direct sound contributions. Double diffraction contributions are much smaller than single diffraction contributions. Diffraction contributions are important for receivers in an acoustical shadow zone. The diffraction contribution is reduced when a receiver is positioned deeper into the acoustical shadow zone (i.e. further down from the roof) or when the frequency is increased. Finally, diffraction contributions over acoustically rigid wedges are usually larger than corresponding contributions over sound absorbing wedges.

GRs are sound absorbing surfaces and can mitigate sound produced by diffraction in the urban environment. Therefore, diffraction contributions over GRs, as compared to conventional acoustically rigid roofs, are smaller and contribute to a quieter urban environment.

5.3.1. Models

The theory of single wedge diffraction is quite developed, and analytical solutions exist for rigid wedges, e.g. Oberhettinger's exact solution for spherical incident signals [184] or various approximate solutions [185,186]. Analytical solutions for diffraction on a sound absorbing right-angled wedge [187] as well as approximate expressions for double edge diffraction [188] also exist. Semi-empirical formulas for single or double diffraction and rigid or sound absorbing wedges are also available [189]. Additionally, numerical methods have been widely employed to account for the combined effects of propagation mechanisms (including diffraction) in complex environments (beam-tracing methods, ray-tracing methods, finite difference time domain models, etc.). The accuracy of all models and solutions depends highly on the accuracy of the sound absorption coefficient of the faces of the wedge (i.e. the GR).

In the problem of sound diffraction over a GR, it is the relative position of source-green roof-receiver that determines the sound field in the shadow zone past a GR. In general, the higher the frequency and the deeper into the shadow zone the receiver is located, the longer the propagation path interacts with the GR, and the better the noise shielding is. The final benefit of a GR also depends on its sound absorbing performance, and thus on water content, vegetation coverage, etc., as discussed in the previous section.

5.3.2. Experimental evidence

Yang at el [190]. conducted measurements in an anechoic chamber for GR systems on a low-profiled structure at street level, such as above underground parking lots. The sound field attenuation in the shadow region increased as the number of rows of the green roof trays grew. Compared to empty trays, the extra sound field attenuation caused by substrates can be up to 9.5 dB at certain frequencies. The depth and type of substrate did not play a significant role. Prune leaves improved the noise shielding at high frequencies.

Van Renterghem and Botteldooren [191] carried out in-situ measurements before and after the placement of GRs for various geometry configurations involving single and double diffraction. It was shown that, compared to non-vegetated roofs, GRs can reduce the noise levels at receivers in the shadow zone, and thus improve the shielding effect of buildings. A single diffraction configuration resulted in an improvement above 10 dB in the shielding effect for frequencies between 400 Hz and 1250 Hz. In other cases, GRs improved while in others deteriorated the shielding provided by non-vegetated roofs, depending on the frequency. A double diffraction configuration yielded up to 8 dB of improvement. For double diffraction cases, the GR improvement was less frequency-dependent. Furthermore, results showed that the extra benefit of a GR (compared to a non-vegetated roof) is stronger for receivers deeper into the shadow zone. It was also reported that for high frequencies, a small substrate thickness and/or the presence of vegetation seems to be positive, while for low frequencies a thicker substrate seemed to be required.

5.3.3. Parameters

Van Renterghem and Botteldooren [192] conducted an in-situ experiment involving single edge diffraction with an extensive GR exposed to natural precipitation. It was shown that, for frequencies between 250 and 1250 Hz, sound diffraction was especially sensitive to the substrate's volumetric water content. The difference in the GR's noise attenuation between a relatively dry and fully saturated state varied by up to 10 dB. Other parameters that affected the sound absorbing characteristics of the GR, such as the thickness of the substrate and the fraction of the roof coverage, have been studied numerically for the diffraction problem [193] as well as, in the case of a diffraction-specific parameter, the shape of the roof [194].

6. Life cycle assessment of green roof systems

According to the ISO 14040 and 14044 standards, life cycle assessment (LCA) studies are generally conducted in four distinct phases. Goal and scope definition is the first step of the analysis. In the majority of published studies, the lifespan of a GR was set to be between 40 and 50 years [54,195–203]. The functional unit differed among the reviewed studies, with the most common being one square meter of roof area and others examining the area of the entire building roof [195,198,199,201,202]. The system boundary incorporates the extraction of raw materials, fabrication of GR layers, transportation, assembly, operation, and disposal or recycling of GR components. In only two papers [195,204] the boundary was set from cradle to gate, excluding the use and end-of-life phases. Several studies performed LCA of GRs from cradle to grave, with the end of life cycle being disposal [205,206] and/or recycling [54,195,196,200,202,207]. Other studies included specific phases of the entire GR [54,198,200,205] or GR layers [54,208].

Life Cycle Inventory Analysis (LCIA) was the subject of investigation in the second step of the assessment. Among the reviewed studies, 70.6% used the ecoinvent database (https://ecoinvent.org/) [54,195–198,200,204,205,207–210]. In life cycle impact assessment, the focus of the study determines the chosen assessment methodology. All of the articles assessed in this review presented (at least) the CO_2 emissions or Global Warming potential (GWP) or Carbon footprint of the examined GRs or the GR layers. In many cases, several other impact categories were also included, i.e. human health, ecosystem quality, climate change, resources, photochemical ozone creation, abiotic depletion potential, and eutrophication potential [195,197,198,203]. An LCA is concluded with the interpretation of results so that a more informed decision may be made [211].

While GRs provide additional environmental benefits and have proved to be more sustainable options for urban planning compared to conventional roofs, some authors have reported that GRs have greater or nearly the same environmental impacts as conventional roofs. It has been argued and substantiated that with a 53% lower contribution in the respiratory organics impact category, EGRs result in a lower environmental impact than TGBRs [195]. Other studies have demonstrated that EGRs perform better than TGBRs for almost all impact categories, excluding carcinogens and water scarcity [201]. Compared to flat roofs, it has been shown that they have a more favorable environmental footprint, in particular with lower values for embodied energy, GHG emissions, and waste material. These savings vary from 55 to 28% for EGRs and IGRs respectively [199]. Another study assessed four main impact categories: human health, ecosystem quality, climate change and resources, with steel and concrete being the most polluting components for both THRs and EGR. Due to the fact that EGR is a more complicated technology, the emitted CO_2 was primarily affected by the thermal insulation material, the root barrier, and the asphalt component. The environmental impacts CO_2 emissions, human health, ecosystem quality, and also resources in both studied roofs were significantly reduced [198]. Other research found that GRs may reduce environmental impacts, particularly during the use phase, but this effect is offset by the increase in additional layers over their construction [203].

This review considers all life cycle phases of the investigated products as well as their environmental impacts. Table 7 provides an overview of LCA studies of GRs, reporting on the kind of study (comparison, or case study), type of investigated GR (EGR, IGR, SIGR or conventional roof) or GR layers (root barrier or substrate), chosen life span, functional unit, and system boundary, along with the environmental impact categories, methods and the corresponding key outcomes.

The phases of materials production and roof construction dominated the environmental impacts of the studied roof assemblies. The manufacture of low density polyethylene and polypropylene as well as the polyethylene of extruded polystyrene had significant environmental impacts [54,204]. The manufacture of polymers required substantial amounts of energy, which had a detrimental impact on climate change, while NO_2, SO_2, O_3 and PM_{10} emissions were major pollutants [54,205]. It is worth mentioning that the primary input for the fabrication of polyester was the felt for irrigation [204]. The production of cement was the dominant factor in global warming potential, resource consumption, and human toxicity [209]. While, the fabrication of hydroponic mineral wool had the greatest environmental impacts, it was shown that using this element as a substrate replacement reduced the impacts of the use phase, concluding that the current material was similar to natural substrates [210]. Likewise [202], revealed a negative value of the same element, contributing to carbon storage in the production of drainage layer in GR-a.

However, while for all the roof elements, the uppermost burdens (impacts) raised from the production stage in the case of clay tiled roof, impacts mainly came from clay bricks, tiles, and concrete due to the use of non-renewable primary energy in the furnace and the consumption of natural resources [197]. The fabrication processes of the materials that composed a roof, accounted for more than half of the roof's global environmental impacts across all categories. Specific values such as 95, 90, 90, 80 and 70% were noted for freshwater aquatic ecotoxicity, marine aquatic ecotoxicity, terrestrial ecotoxicity, photochemical oxidation, and eutrophication, respectively [204].

In the transportation phase, it was identified that IGRs were affected eight times more than EGRs in all impact categories [209]. Other outputs showed that, due to the energy class of the transport trucks, the categories of climate change and human health were highly impacted in the case of bituminous membrane, culture and vegetated layer respectively [205]. Locally produced materials for the studied substrates were beneficial [200]. Findings at the assembly level showed that ready mixed concrete, reinforced metal bars, and mastic asphalt were the most significant contributors to the environmental profile of TGBR and EGR, polluting the drainage layer and vegetation in the case of EGRs [8].

Compared to conventional roofs, all types of GRs had decreased CO_2 emissions during the installation stage [199]. In IGRs, the global warming potential was largely driven by the increased quantities of concrete used. The IGR was the most impacting roof for all use phases considered [195,209], whereas the impact of TGBR and EGRs was largely determined by the use phase and the roof components [201]. Regarding global warming, a remarkable decrease of 73.3 and 75.74% occurred in R_2 and R_3 compared to R_1, resulting from the reduction in the energy consumption of the use phase, once the roof was well insulated [206]. Using rockwool as a substrate in GRs, resulted in energy savings and an equivalent reduction in CO_2 emissions [200]. Using a brick substrate could reduce the global warming potential to 3139 kg CO_2eq, whereas cork drainage could reduce it to 441 kg CO2eq. Both the GR-c and GR-a configurations had equivalent use stages, but plant CO_2 fixation reduced the GWP significantly to 6828 kgCO_2eq [202]. Another study found that while ozone depletion increased by 1.3% during the use phase of the studied GR, all other environmental impact categories decreased [203]. On the other hand, the usage of layers made out of recycled polymers resulted in lower values, avoiding toxic air emissions in all studied scenarios [54]. Similarly, other studies found that GRs had greater LCA values than white roofs in the materials production, construction process, and end-of-life stages [195,203].

For end-of-life scenarios (recycling and landfilling) and for both TGBR and EGRs, the emissions of SO_2 and NO from a grid connected to an oil powered plant had a considerable effect on the aquatic and terrestrial acidification impact categories. In addition, during the recycling phase of the aluminum screws in the thermal insulation layer, TGBRs released carcinogenic aromatic hydrocarbons and benzo[a]pyrene into the atmosphere [201]. Another critical finding was that NO_2 was removed from the air rather than released during the recycling process of a GR [54]. The recycling potential for the drainage layers of GR-c and GR-a had GWP reductions of 643 and 846 kgCO_2eq, respectively. The same roofs scored 32 and 55% of the GWP during the demolition phase [202]. On the other hand, the byproduct evaluation approach had a significant impact when layers from a nature-based

Table 7
Cited studies addressing LCA and environmental aspects of GRs.

Reference	Type of study	Type of green roof	Region/country	Life span (yr)	Functional unit	System boundaries	Studied environmental impact categories and methods	Main results/ environmental impacts
[195]	Comparison	EGR, IGR, TGBR, and WRR	Lebanon	45	834 m^2 of GR	Cradle to gate	Human health, ecosystem quality, climate change, resources IMPACT 2002+	EGRs had a better environmental performance for all the examined impact categories. Compared to other roofs, IGRs resulted in the worst values for carcinogens, ionizing radiation, ozone layer depletion, aquatic eutrophication, global warming, and non-renewable energy impact categories, while WRRs scored the highest values at the rest of the impact categories.
[54]	Comparison	EGR, IGR	–	40–50	Production of 1 kg of polymer	Manufacturing and construction	Eco-Indicator (H) v2.06	The total pollutants that resulted showed that non-recycled LDPE released 2.8 times more toxic elements to the air than recycled LDPE. If 100% (rather than 40%) recycled PP was used in the drainage layer, a significant pollution reduction would be achieved.
[196]	Comparison	Two lightweight EGRs	Helsinki, Finland	40	1 m^2 of GR	Cradle to grave	CML 2001	The second substrate (root barrier with LPDE) performed better than the first one (root barrier with PVC). This was largely due to the production of expanded clay in the first substrate, which emitted 48% more GWP100 than the second substrate.
[197]	Comparison	4 different GRs compared to a standard clay pitched roof	Pisa, Italy	40	1 m^2 of GR	Cradle to grave	CML-IA v4.1	All four studied GRs scored lower impacts than the clay pitched roof, mainly ADP-fossil fuels (20–30%) and ODP (5–6%), whereas the typical decrease was 5% for all other impact categories, except POCP (1%) and GWP (2%).
[198]	Comparison	THR and EGR	Thessaloniki, Greece	15 for THR and 45 for EGR	69.271 m^2	Construction, transportation and energy use for the construction and reservation of both roofs	Human health, ecosystem quality, climate change and resources	Both THR and EGR roofs had similar reductions of 61%, 23%, 11% and 10.5% to climate change, human health, ecosystem quality, and resources respectively.
[199]	Comparison	EGR, IGR, SIGR, and flat roofs	4 Greek cities: Heraklion, Athens, Thessaloniki, and Florina	40 for GRs and 20 for flat roofs	100 m^2 of roof area	Cradle to grave	–	Compared to flat roofs, GRs showed important decreases such as 24–32% and 15–60% in CO_2 emissions and waste production respectively. An impressive increase of 279–835% was observed in total life cycle water consumption, due to high irrigation needs.

(*continued on next page*)

Table 7 (*continued*)

Reference	Type of study	Type of green roof	Region/country	Life span (yr)	Functional unit	System boundaries	Studied environmental impact categories and methods	Main results/ environmental impacts
[200]	Comparison	EGR and SIGR	Athens, Greece	40	–	Construction, transportation and use phase	Carbon footprint	The computation of total CO_2 emissions (in kg CO_2et^{-1}) used the means of the intervals 236.6−264.6 and 1544.0−1584.0 for the coarse aggregate synthesis, and the high-density rockwool respectively.
[201]	Comparison	TGBR and EGR	Lebanon	15 for TGBR and 45 for EGR	Installation and use of a 650 m^2 roofing system for 1 year	Cradle to grave	Water scarcity (WULCA) IMPACT 2002+	EGRs had a better environmental performance compared to TGBRs for almost all impact categories. The total water scarcity scored 53.3 and 54.5% for TGBRs and EGRs, respectively.
[208]	Case study	A bituminous anti-root barrier on a GR	Calabria, Italy	–	1 kg of hot-worked adhesive bitumen membrane	Production, transportation, operation and disposal of bitumen membranes	ReCiPe endpoint impact 2002+	As bitumen encloses sulfur compounds it could develop small amounts of toxic sulfur gaseous such as hydrogen sulfide (H_2S). An increase of the useful life of the membrane is essential.
[205]	Case study	GRWRS	Calabria, Italy	–	1 m^3 of the stratigraphy of GRWRS	Raw materials extraction, production, and transportation from the supplier to the installation place; and energy consumption linked to the transformation	Impact 2002+	The total climate change impact comes to 17.4, 18.2, 18.7, 18.3, 13.78 and 13.5% referring to the contribution of the layers anti-root bituminous membrane, water storage, drainage, filter, culture-vegetated respectively.
[209]	Comparison	A lightweight EGR and a heavyweight IGR	Antananarivo, Madagascar	1, 5 and 10	Construction, transmission and use of 1 m^2 of GR for a period of 1, 5 and 10 years	Extraction of raw materials, energy conversion-supply, manufacture transport, and waste production during the manufacture of various layers and use of the studied GRs	CML baseline	At the production phase, cement emitted 53 kg of CO_2eq more than wood, with steel causing only 5.3 kg of CO_2eq of additional burdens.
[207]	Comparison	4 types of EGR	Israel	20	1 m^2 of roof area	Cradle-to-grave (no use phase included)	ReCiPe	The corresponding values in the production and end-of-life phase were equal to 88−94% and 6−12% along with 93–94% and 6−7% of total LCA in the mass allocation and system expansion approach respectively.
[204]	Comparison	An ecological roof in 5 winter climate contexts	Cádiz, Valencia, Vigo, Madrid and Soria (Spain)	–	1 m^2 of ecological roof	Cradle to gate	CML 2000	The structural support materials contributed 95, 90, 90, 80 and 70% freshwater aquatic ecotoxicity, marine aquatic ecotoxicity, terrestrial ecotoxicity, photochemical oxidation, and eutrophication, respectively.
[206]	Comparison	R_1: simple roof; R_2: typical reversed roof; and R_3: GR	Salerno, Italy	–	1 m^2 of roof area	Cradle to grave	Eco-indicator 99	R_1, R_2, and R_3 resulted into a total damage of almost 106.83, 32.62, and 33.14 Pt respectively. Damage

(*continued on next page*)

Table 7 (*continued*)

Reference	Type of study	Type of green roof	Region/country	Life span (yr)	Functional unit	System boundaries	Studied environmental impact categories and methods	Main results/ environmental impacts
								categories included respiratory inorganics, caused by the particulate matter emitted during the transportation and extraction of materials. The climate change category was decreased, due to the vast reduction in consumed energy in the use phase. In R_2, the disposal scenario of a specific plastic layer increased the percentage of carcinogens in comparison to the other roofs.
[202]	Comparison	GR-c and GR-a	Germany	40	218 m^2 of GR	Cradle to grave	–	In the production phase, the GWP had a higher impact on the GR-c, with 3,617, 998, 774, and 275 kg CO_2eq for the substrate, PP-drainage PVC-root barrier, filter layer, and protection layer respectively. For the GR-a, the GWP values were 53 and −2112 kg CO_2eq for the substrate and drainage layer respectively. The filter and protection layers of both roofs decreased GWP by 186 kgCO_2eq, while the root barrier saved another 219 kgCO_2eq.
[210]	Comparison	4 SIGRs	Czech Republic	20	1 m^2 of roof area	Cradle to grave	CML 2001	Among the materials used, the environmental impacts of Assemblies 1 and 2 were such that the intensive substrate mixture was responsible for −65.68 and 41.64% respectively; in Assemblies 3 and 4, the HMW was 49.80 and 79.98% respectively.
[203]	Comparison	Conventional white roof EGR	Florida, US	50	–	Cradle to grave	Global warming potential, acidification potential, human health, particulate, eutrophication potential, ozone depletion potential and smog potential	GWP for a conventional white roof and GR decreased by 9.4% and 8.58%; 3.28% and 3.16%; −0.65% and −0.66%; 2.64% and 2.57%, in the categories of material production, construction process, and use and end of life, respectively.

material (perlite) were replaced by byproducts of the CBA and FAAs layers [207]. When recycled materials replaced virgin ones, drainage and water retention improved [196].

It is worth noting that Peri et al. [212] discuss the challenges of disposing of green roofs at the end of their lifecycle. The authors address the lack of regulations and guidelines for the disposal of green roofs and propose an "Allowed by legislation" end-of-life scenario that considers the current waste management regulations and practices. They also suggest a methodology for assessing the environmental impact of different disposal scenarios. The study found that the environmental impact of green roof disposal depends on several factors, such as the type of vegetation, substrate, and waste management practices. The authors conclude that adopting an "Allowed by legislation" end-of-life scenario and conducting a thorough environmental analysis can help facilitate the sustainable disposal of green roofs and minimize their environmental impact. Overall, the article offers valuable insights into the need

for proper disposal practices for green roofs and the importance of considering environmental impact when designing and implementing sustainable solutions.

The different phases of a GR were also compared. The production and end-of-life phases saved impacts significantly more than the use phase because they were capable of extending the roof's component life cycle, achieving a longevity for 20 years [199]. Maiolo et al. [205] analyzed a bituminous anti-root barrier on the GR of a building in the University of Calabria in Southern Italy. The phases of extracting raw materials and using non-renewable primary energy had a negative impact on the category of resources. CO_2 emissions had the most significant impact when compared to the outputs of the two methods used (ReCiPe Endpoint and Impact 2002+) [205].

According to Rivela et al. [204], the used structural support was regarded as a common component of an examined ecological roof, so it was not taken into account in the comparative analysis. The elements identified as major contributors to the global warming category were the insulation and surface finish subsystems. The first subsystem decreased significantly the impacts of ozone layer depletion, global warming, abiotic depletion, acidification and photochemical oxidation, by 95, 55, 55, 50, and 45% respectively. The second subsystem contributed the most to the categories of human toxicity (65%), marine aquatic ecotoxicity (around 45%), and terrestrial ecotoxicity (around 45%) [204]. On the other hand, Pushkar claimed that with the mass allocation method, the replacement of nature-based material layers (perlite) with CBA and FAAs byproducts in the substrate and drainage layers, was environmentally damaging with impacts ranging from 5 to 20% of the total impacts. On the other hand, the system expansion approach was advantageous for the same procedure, with lower values of around 20–40% [207].

Wrapping up this section, Table 7, which summarized the GR LCA review, demonstrates that all major LCA indicators of a GR were significant smaller than those of conventional structural elements. The replacement of the substrates and finishing subsystems with recycled and eco-friendly materials underscores the recent trend in the GR industry to minimize environmental impacts and contribute to the circular economy.

7. The role of plants and water scarcity issue

Recognizing the role of plants in shielding a roof from direct sunlight, absorbing some precipitation water, and cooling off the roof surface, it may be concluded that the use of plants on a roof improves its functionality, aesthetics, and the buildings surroundings [59,102,213]. GRs are living systems, and the selection criteria for plant species play a crucial role in their effective function, even if the selection is not typically driven by ecological criteria or made according to the structural characteristics of the plants [214].

Depending on the type of GR (extensive, semi-intensive or intensive), native or alien plants, species with different functional traits (annual, perennial, succulent or not, shrub or herb, etc.) and specific structural characteristics (such as root growth, which can constitute a risk for the structural integrity of roofs) could be selected. This is due to the fact that on intensive roofs, plants require regular and frequent maintenance, while on extensive roofs, plants are often selected from a limited set of species (as suggested by the literature). As an example, it is recommended to avoid using (a) woody plant species (such as Phanerophytes), because they typically have a well-developed root system, which can damage the layers of the roof isolation over time, and (b) annual plants (such as Therophytes) and biennial Hemicryptophytes, because they are short lived and thus do not provide a continuous cover for green roofs.

Since native plants (a) are better adapted to the prevailing bioclimatic conditions in each study area, (b) provide greater environmental benefits, and (c) are more aesthetically pleasing than non-native plants, their use has garnered considerable attention in recent years [215].

A study is required for the proper selection of plants based on synecological, structural, chorological, and autoecological criteria. For example, in order to select plants in Italy, synecological information derived from studies on natural plant communities were used initially [216], followed by a final selection of species typical of habitats with affinity to the conditions of the specific roof. It has been suggested to select plants that are typical of early successional communities of the Mediterranean and capable of colonizing thin (not mature) and compact substrates, such as rocks, walls, screes, and dunes. It has been established experimentally that the usage of various plant species on GRs is preferable to monocultures [217]. Consequently, the selection of a single species or a mix of species is a crucial element of the evaluation and selection of plants.

Depending on the climatic area, the chorology of plants (origin and current area of native distribution) should be used as a selection criterion to consider the exclusion of alpine, boreal, and mountain species, e.g. for a GR in the Mediterranean. Caneva et al. [214] excluded endemic species from the list of potential plants, due to their generally narrow ecological requirements. One more important selection criterion mentioned in Suszanowicz et al. [218] is related to the protection and enhancement of biodiversity in urban areas, through the reintroduction of native plant species occurring in the urban/semi-urban and wider neighboring areas that can be used on GRs (with resistance to stress caused by large temperature differences in the summer and the winter, long dry periods, or torrential rains).

According to Monteiro et al. [219], an interesting case is to identify aromatic plants that could be used successfully in GRs in Mediterranean climates, where extended drought periods in the summer contrast with cold and wet winter periods.

It is obvious that the proper functioning of a green roof system is based on the consumption of water not only for the survival of the plants but also for the improvement of its properties related to the energy savings of the building. Water scarcity has become a real problem due to the combination of climate change and population explosion. According to the IPCC report on "Climate Change 2022: Impacts, Adaptation and Vulnerability" [220], risks in water availability and will continue to increase by the mid-to long-term. The solution is the adaptability to the aforementioned risks and this affects the design of green roofs. The ultimate goal is to reduce potable water for irrigation.

Water consumption in a green roof system depends on the type of roof (intensive, extensive), on the used plants, such as the drought resistant species of Sedum, the growing medium, and finally the irrigation method together with the proper design of the retention layers. Low volume drip irrigation can lower water consumption considerably. The analysis presented by Pirouz et al. [221] showed that the average water use of green roofs in the summer (in humid regions) is about 3.7 $L/m^2/day$, in Mediterranean regions about 4.5 $L/m^2/day$, and in arid regions about 2.7 $L/m^2/day$.

The authors proposed a new GR system that will take advantage of water from fog or dew. In arid areas, fog potential is between 1.8 and 11.8 $L/m^2/day$ while dew potential ranges from 0.5 to 0.7 $L/m^2/day$, reducing the dependency on urban water infrastructure. In addition there are ways to recover condensed water from HVAC systems [222], which can be used for irrigation. Fortunately, there are additional ways that can close the gap between the irrigation requirements of a green roof and the simultaneous reduction of potable water consumption. This way, the advantages of a green roof in a building's energy balance are maintained without burdening its water balance. The collection of rainwater, the reuse of grey water and desalination (where this is possible, especially using solar radiation) are important climate change adaptation measures, turning green roofs into profitable investments even in areas with potable water availability problem.

8. Engineering perspectives and future directions

Researchers have concentrated their attention on particular aspects of GRs, assessing their effectiveness primarily in connection to the

energy economy in well-defined areas and situations. However, nature does not isolate, but rather functions synthetically in multicomponent and multidimensional directions. When integrating nature-inspired solutions, various components complement one another. For example, improving energy efficiency and ameliorating environmental impacts through the use of GRs, has a positive effect on the well-being and health of people. Moreover, the reduction of carbon emissions and the sequestration of carbon by GRs play a key part in climate neutrality.

Another significant benefit of GRs is that they do not generate solid waste at the end of their lifetime. Neither do they emit organic pollutants during their active life. Unlike other synthetic polymers and resins used in insulation materials, the construction of GRs does not involve polluting and energy-intensive industrial processes. The life cycle assessment of GRs demonstrates that they have a lower lifetime environmental impact than conventional insulation materials. Although incorporating insulation into buildings has become a high priority, the life cycle of insulation materials and how they contribute to the circular economy has received little consideration. Therefore, policymakers and stakeholders should prioritize the incorporation of GRs in the engineering options for the thermal shielding of buildings.

GRs are an excellent component of the urban environment that can be implemented directly. Synergies with other technologies (such as cool materials, heating, ventilation and air-conditioning, blue infrastructure, green walls, etc.), which can increase the overall effectiveness of GRs and improve other aspects of the urban environment, should be exploited.

As demonstrated by this review, the efficiency of a GR depends on several factors. The type of GR, the plants utilized, potential combination with water or green walls, local climate conditions, and building materials, all affect the outcome. Moreover, a larger GR is expected to be more efficient than a smaller one, given the importance of end effects in heat transfer. The height of the building also plays a key role: in the case of a tall building, heat absorption by walls can contribute significantly to the thermal resistance of the building. Consequently, choosing a lower height and fewer-story buildings as an architectural alternative in combination with a GR may be viewed as a more integrated solution.

GR applications may be seen from a broader perspective and stimulate research toward discovering synergistic benefits. In terms of energy savings, GRs do not contribute significantly to winter heating needs. However, their contribution to reducing point source pollution should be considered and researched. Combined systems should be designed and implemented to purify the flue gas emissions from a building's HVAC systems. Those gases can be scrubbed using a closed recirculation water system that runs through appropriately chosen aquatic plants in a water pond of a GR complex.

Making area-specific choices, exploiting local plants that adapt better to local climate conditions, and even picking them to preserve local biodiversity, may be excellent synergistic options. Creating roof gardens, where flowers and vegetables are cultivated, or planting fruit trees on a GR are further examples of the combination of GRs with the phototherapeutic advantages of horticulture. Research on the plants that are best suited to GR applications, absorb specific pollutants, and provide more efficient shading, can offer additional benefits, and should be explored.

9. Conclusions

GRs are nature-based solutions that are designed and implemented as artificial ecosystems to reduce energy consumption, improve air quality, and promote urban sustainability. This manuscript is a bibliographic review of the leading scientific processes, models, and optimization methods describing the thermal performance of a GR holistically. The review process is complemented with a comprehensive description of the primary system benefits, including energy and environmental aspects. At the same time, it concludes with a thorough review of life cycle assessment in order to provide a useful summary of the environmental impacts of GR systems. This review demonstrates the effectiveness of GRs in various ways. It becomes apparent that GRs can serve several purposes. It was demonstrated that GRs can regulate indoor temperatures by lowering cooling energy demand during the summer and heating energy consumption during the winter, while also contributing measurable reductions in noise, local atmospheric pollution, and water runoff.

Concluding remarks are summarized as follows:

(1) Modelling the thermal performance of GR system: energy models were classified into three categories according to the methodology used: models based on thermal transmittance coefficient calculation, models based on energy balance calculation at various levels and components of the system, and data-driven models.
(2) Parametric studies: Several system parameters were considered such as LAI, soil layer thickness, insulation thickness, irrigation, foliage height and density, type of planted roof, plant coverage, etc. Among them, LAI was found the parameter affecting more considerably the thermal behaviour of the GR system.
(3) Energy benefits: GRs contribute to a significant reduction of cooling load reaching up to 70% as well as to a decrease of indoor temperature up to 15 °C.
(4) Environmental benefits: GRs environmental benefits included air pollutants concentration reduction $PM_{2.5}$, PM_{10}, O_3, SO_2, NO_2; carbon sequestration through photosynthesis and evapotranspiration; runoff water quality improvement; and urban noise reduction. Experiments and observations showed 7–33% reduction of $PM_{2.5}$, and significant reduction in PM_{10}, O_3, NO_2, while GRs showed an excellent contribution to carbon sequestration.
(5) Life Cycle Assessment: The LCA review showed that all major LCA indicators of a GR were smaller than those of conventional structural elements.

In closing, the present manuscript provides: (a) a holistic and interdisciplinary review of the subject offering a global perception of the related information, (b) a critical discussion of several individual aspects such as system benefits, and (c) perspectives able to fill the research gap between scientific foundation and engineering thinking that may be applied and implemented.

Declaration of competing interest

The authors declare that they have no known competing financial interests or personal relationships that could have appeared to influence the work reported in this paper.

Data availability

No data was used for the research described in the article.

Acknowledgments

The authors thank the journals that permitted the use of Figs. 1 and 2. The publication fees of this manuscript have been financed by the Research Council of the University of Patras.

References

[1] Cook LM, Larsen TA. Towards a performance-based approach for multifunctional green roofs: an interdisciplinary review. Build Environ 2021;188:107489.
[2] Liu H, Kong F, Yin H, Middel A, Zheng X, Huang J, et al. Impacts of green roofs on water, temperature, and air quality: a bibliometric review. Build Environ 2021; 196:107794.
[3] Espinosa-Paredes SQ-GG, Polo-Labarrios MA, Espinosa-Martínez EG, Escobedo-Izquierdo MA. Green roof heat and mass transfer mathematical models: a review, Building and Environment. Build Environ 2020;170:106634.

[4] Williams KJH, Lee KE, Sargent L, Johnson KA, Rayner J, Farrell C, et al. Appraising the psychological benefits of green roofs for city residents and workers. Urban For Urban Green 2019;44:126399.
[5] Shafique M, Kim R, Rafiq N. Green roof benefits, opportunities and challenges-A review. Renew Sustain Energy Rev 2018;90:757–73.
[6] Ferrante A, Mihalakakou G. The influence of water, green and selected passive techniques on the rehabilitation of historical industrial buildings in urban areas. Sol Energy 2001;70:245–53. https://doi.org/10.1016/S0038-092X(00)00100-6.
[7] Raji B, Tenpierik MJ, Dobbelsteen A. The impact of greening systems on building energy performance: a literature review. Renew Sustain Energy Rev 2015;45:610–23.
[8] Susca T, Gaffin SR, Dell'Osso GR. Positive effects of vegetation: urban heat island and green roofs. Environ Pollut 2011;159:2119–26.
[9] Chen D, Wang X, Thatcher M, Barnett G, Kachenko A, Prince R. Urban vegetation for reducing heat related mortality. Environ Pollut 2014;192:275–84.
[10] Felson AJ, Oldfield EE, Bradford MA. Involving ecologists in shaping largescale green infrastructure projects. Bioscience 2013;63:882–90.
[11] Demuzere M, Orru K, Heidrich O, Olazabal E, Geneletti D, Orru H, et al. Mitigating and adapting to climate change: multifunctional and multi-scale assessment of green urban infrastructure. J Environ Manag 2014;146:107–15.
[12] Susca T. Green roofs to reduce building energy use? A review on key structural factors of green roofs and their effects on urban climate. Build Environ 2019;162:106273.
[13] Mihalakakou G, Papadaki MSM, Halkos G, Paravantis J, Makridis S, Papaefthymiou S. Applications of earth-to air heat exchangers: a holistic review. Renew Sustain Energy Rev 2022.
[14] Santamouris M. Cooling the cities – a review of reflective and green roof mitigation technologies to fight heat island and improve comfort in urban environments. Sol Energy 2014;103:682–703.
[15] Mihalakakou G, Flocas HA, Santamouris M, Helmis CG. Application of neural networks to the simulation of the heat island over Athens, Greece, using synoptic types as a predictor. J Appl Meteorol 2002;41:519–27.
[16] Mihalakakou G, Santamouris M, Papanikolaou N, Cartalis C, Tsangrassoulis A. Simulation of the urban heat island phenomenon in Mediterranean climates. J Pure Appl Geophys 2004;161:429–51.
[17] Vera S, Pinto C, Tabares-Velasco PC, Bustamante W. A critical review of heat and mass transfer in vegetative roof models used in building energy and urban environment simulation tools. Appl Energy 2018;232:752–64.
[18] ESPON. Shrinking rural regions in Europe towards smart and innovative approaches to regional development challenges in depopulating rural regions n.d.
[19] Berardi U, Hoseini AHG, GhaffarianHoseini A. State-of-the-art analysis of the environmental benefits of green roofs. Appl Energy 2014;115:411–28.
[20] Karteris M, Theodoridou I, Mallinis G, Tsiros E, Karteris A. Towards a green sustainable strategy for Mediterranean cities: assessing the benefits of large-scale green roofs implementation in Thessaloniki, Northern Greece, using environmental modelling, GIS and very high spatial resolution remote sensing data. Renew Sustain Energy Rev 2016;58:510–25.
[21] Kolokotsa D, Lilli AA, Lilli MA, Nikolaidis NP. On the impact of nature-based solutions on citizens' health & well being. Energy Build 2020;229:110527. https://doi.org/10.1016/j.enbuild.2020.110527.
[22] Vijayaraghavan K. Green roofs: a critical review on the role of components, benefits, limitations and trends. Renew Sustain Energy Rev 2016;57:740–52.
[23] Saadatian O, Sopian K, Salleh E, Lim CH, Riffat S, Saadatian E, et al. A review of energy aspects of green roofs. Renew Sustain Energy Rev 2013;23:155–68.
[24] Williams NSG, Rayner JP, Raynor KJ. Green roofs for a wide brown land: opportunities and barriers for rooftop greening in Australia. Urban For Urban Green 2010;9:245–51.
[25] Castleton HF, Stovin V, Beck SBM, Davison JB. Green roofs; building energy savings and the potential for retrofit. Energy Build 2010;42:1582–91.
[26] Niachou A, Papakonstantinou K, Santamouris M, Tsagrassoulis A, Mihalakakou G. Analysis of the green roof thermal properties and investigation of its energy performance. Energy Build 2001;33:719–29.
[27] Wong NH, Cheong DKW, Yan H, Soh J, Ong CL, Sia A. The effects of roof top garden on energy consumption of a commercial building in Singapore. Energy Build 2003;35:353–64.
[28] Santamouris M, Pavlou C, Doukas P, Mihalakakou G, Synnefa A, Hatzibiros A, et al. Investigating and analysing the energy and environmental performance of an experimental green roof system installed in a nursery school building in Athens, Greece. Energy 2007;32:1781–8.
[29] Alexandri E, Jones P. Developing a one-dimensional heat and mass transfer algorithm for describing the effect of green roofs on the built environment: comparison with experimental results. Build Environ 2007;42:2835–49.
[30] Spala A, Bagiorgas HS, Assimakopoulos MN, Kalavrouziotis J, Matthopoulos D, Mihalakakou G. On the green roof system. Selection, state of the art and energy potential. Renew Energy 2008;33:173–7.
[31] Jaffal I, Ouldboukhitine SE, Belarbi R. A comprehensive study of the impact of green roofs on building energy performance. Renew Energy 2012;43:157–64.
[32] Pandey S, Hindoliya DA. Ritu mod, Artificial neural network for predation of cooling load reduction using green roof over building in Sustainable city. Sustain Cities Soc 2012;3:37–45.
[33] Kolokotsa D, Santamouris M, Zerefos SC. Green and cool roofs' urban heat island potential in European climates for office buildings under free floating conditions. Sol Energy 2013;95:118–30.
[34] Kumar R, Kaushik SC. Performance evaluation of green roof and shading for thermal protection of buildings. Build Environ 2005;40:1505–11.
[35] Liu M. Probabilistic prediction of green roof energy performance under parameter uncertainty. Energy 2014;77:667–74.
[36] Alcazar SS, Olivieri F, Neila J. Green roofs: experimental and analytical study of its potential for urban microclimate regulation in Mediterranean-continental climates. Urban Clim 2016;17:304–17.
[37] Tomson M, Kumar P, Barwise Y, Perez P, Forehead H, French K, et al. Green infrastructure for air quality improvement in street canyons. Environ Int 2021;146:106288.
[38] Pugh TAM, MacKenzie AR, Whyatt JD, Hewitt CN. Effectiveness of green infrastructure for improvement of air quality in urban street canyons. Environ Sci Technol 2012;46:7692–9.
[39] Seyedabadi R, Eicker U, Karimi S. Plant selection for green roofs and their impact on carbon sequestration and the building carbon footprint. Environ Chall 2021;4:100119.
[40] Berndtsson JC, Bengtsson L, Jinno K. Runoff water quality from intensive and extensive vegetated roofs Justyna. Ecol Eng 2009;35:369–80.
[41] Gong Y, Zhang X, Li J, Fang X, Yin D, Xie P, et al. Factors affecting the ability of extensive green roofs to reduce nutrient pollutants in rainfall runoff. Sci Total Environ 2020;732:139248.
[42] Liu W, Wei W, Chen W, Deo RC, Si J, Xi H, et al. The impacts of substrate and vegetation on stormwater runoff quality from extensive green roof. J Hydrol 2019;576:575–82.
[43] Cristiano E, Deidda R, Viola F. The role of green roofs in urban Water-Energy-Food-Ecosystem nexus: a review. Sci Total Environ 2021;756:143876.
[44] Pauleit S, Andersson E, Anton B, Buijs A, Haase D, Hansen R, et al. Urban green infrastructure – connecting people and nature for sustainable cities. Urban For Urban Green 2019;40:1–3. https://doi.org/10.1016/j.ufug.2019.04.007.
[45] Zhang X, Shen L, Tam VWY, Lee WWY. Barriers to implement extensive green roof systems: a Hong Kong study. Renew Sustain Energy Rev 2011;16:314–9.
[46] Feng C, Meng Q, Zhang Y. Theoretical and experimental analysis of the energy balance of extensive green roofs. Energy Build 2010;42:959–65.
[47] Stella P, Personne E. Effects of conventional, extensive and semi-intensive green roofs on building conductive heat fluxes and surface temperatures in winter in Paris. Build. Environ. 2021;205:108202.
[48] Lee LSH, Jim CY. Thermal-irradiance of subtropical intensive green roof in winter and landscape-soil design implications. Energy Build 2020;209:109692.
[49] Cadcone S. Green roof design: state of the art on technology and materials. Sustainability 2019;11:3020.
[50] Vijayaraghavan K, Joshi UM. Can green roof act as a sink for contaminants? A methodological study to evaluate runoff quality from green roofs. Environ Pollut 2014;194:121–9.
[51] Speak AF, Rothwell JJ, Lindley SJ, Smith CL. Urban particulate reduction by four species of green roof vegetation in a UK city. Atmos Environ 2012;61:283–93.
[52] Zhao M, Tabares-Velasco PC, Srebric J, Komarneni S, Berghage R. Effects of plant and substrate selection on thermal performance of green roofs during the summer. Build Environ 2014;78:199–211.
[53] Wong GKL, Jim CY. Quantitative hydrologic performance of extensive green roof under humid-tropical rainfall regime. Ecol Eng 2014;70:366–78.
[54] Bianchini F, Hewage K. How "green" are the green roofs? Lifecycle analysis of green roof materials. Build Environ 2012;48:57–65.
[55] Moody SS, Sailor DJ. Development and application of a building energy performance metric for green roof system. Energy Build 2013;60:262–9.
[56] Abuseif M, Dupre K, Michael RN. The effect of green roof configurations including trees in a subtropical climate: a co-simulation parametric study. J Clean Prod 2021;317:128458.
[57] Carslaw H, Jaeger J. Conduction of heat in solids. second ed. Oxford: Oxford Science Publishers; 1980.
[58] Barrio EPD. Analysis of the green roofs cooling potential in buildings. Energy Build 1998;27:179–93.
[59] Ascione F, Bianco N, de'Rossi F, Turni G, Vanoli GP. Green roofs in European Climates. Are effective solutions for the energy savings in air-conditioning? Appl Energy 2013;104:845–59.
[60] He Y, Lin ES, Tan CL, Tan PY, Wong NH. Quantitative evaluation of plant evapotranspiration effect for green roof in tropical area: a case study in Singapore. Energy Build 2021;241:110973.
[61] Sailor DJ. A green roof model for building energy simulation programs. Energy Build 2008;40:1466–78.
[62] Lazzarin RM, Castellotti F, Busato F. Experimental measurements and numerical modeling of a green roof. Energy Build 2005;37:1260–7.
[63] Ayata T, Tabares-Velasco PC, Srebric J. An investigation of sensible heat fluxes at a green roof in a laboratory setup. Build Environ 2011;46:1851–61.
[64] Jim CY, Tsang SW. Modeling the heat diffusion process in the abiotic layers of green roofs. Energy Build 2011;43:1341–50.
[65] Ouldboukhitine SE, Belarbi R, Sailor DJ. Experimental and numerical investigation of urban street canyons to evaluate the impact of green roof inside and outside buildings. Appl Energy 2014;114:273–82.
[66] Heidarinejad G, Esmaili A. Numerical simulation of dual effect of green roof thermal performance. Energy Convers Manag 2015;106:1418–25.
[67] Refani AH, Talkhabi H. Investigating the effective factors on the reduction of energy consumption in residential buildings with green roofs. Renew Energy 2015;80:595–603.
[68] Chen PY, Li YH, Lo WH, Tung CP. Toward the practicability of a heat transfer model for green roofs. Ecol Eng 2015;74:266–73.
[69] Quezada-García S, Espinosa-Paredes G, Escobedo-Izquierdo MA, Vázquez-Rodríguez A, Vázquez-Rodríguez R, Ambriz-García JJ. Heterogeneous model for heat transfer in green roof systems. Energy Build 2017;139:205–13.

[70] Škerget L, Tadeu A, Brebbia CA. Transient numerical simulation of coupled heat and moisture flow through a green roof. Eng Anal Bound Elem 2018;95:53–68.
[71] Asadi A, Arefi H, Fathipoor H. Simulation of green roofs and their potential mitigating effects on the urban heat island using an artificial neural network: a case study in Austin, Texas. Adv Space Res 2020;66:1846–62.
[72] Wei T, Jim CY, Chen A, Li X. Adjusting soil parameters to improve green roof winter energy performance based on neural-network modeling. Energy Rep 2020; 6:2549–59.
[73] Hirsch JJ, editor. DOE-2 building energy analysis; 1998.
[74] EnergyPlus. simulation software. 2011.
[75] Incropera FP, Dewit DP. Fundamentals of heat and mass transfer. New York: John Wiley & Sons; 2002.
[76] Mazzeo D, Matera N, Peri G, Scaccianoce G. Forecasting green roofs' potential in improving building thermal performance and mitigating urban heat island in the Mediterranean area: an artificial intelligence-based approach. Appl Therm Eng 2023;222:119879. https://doi.org/10.1016/j.applthermaleng.2022.119879.
[77] Yaghoobian N, Srebric J. Influence of plant coverage on the total green roof energy balance and building energy consumption. Energy Build 2015;103:1–13.
[78] Foustalieraki M, Assimakopoulosa MN, Santamouris M, Pangalou H. Energy performance of a medium scale green roof system installed ona commercial building using numerical and experimental datarecorded during the cold period of the year. Energy Build 2017;135:33–8.
[79] Yang J, Kumar DIM, Pyrgou A, Chong A, Santamouris M, Kolokotsa D, et al. Green and cool roofs' urban heat island mitigation potential in tropical climate. Sol Energy 2018;173:597–609.
[80] Solcerova A, F van de V, Wang M, Rijsdijk M, Giesen N. Do green roofs cool the air? Build Environ 2017;111:249–55.
[81] Theodosiou TG. Summer period analysis of the performance of a planted roof as a passive cooling technique. Energy Build 2003;35:909–17.
[82] Roche P, Berardi U. Comfort and energy savings with active green roofs. Energy Build 2014;82:492–504.
[83] Quezada-Garcia S, Espinosa-Paredes G, Vazquez-Rodriguez A, Ambriz-Garcia JJ, Izquierdo AME-. Sensitivity analysis of a green roof. Int J Green Energy 2016;13: 260–6.
[84] Chen J, Rich PM, Gower ST, Norman JM, Plummer S. Leaf area index of boreal forests: theory, techniques, and measurements. J Geophys Res 1997;102: 29,429–29,443.
[85] Jaffal I, Ouldboukhitine SE, Belarbi R. A comprehensive study of the impact of green roofs on building energy performance. Renew Energy 2012;43:157–64.
[86] Akbari H, Menon S, Rosenfeld A. Global cooling: increasing world-wide urban albedos to offset CO 2. Climatic Change 2009;94:275–86.
[87] Akbari H, Rose LS, Taha H. Analyzing the land cover of an urban environment using high-resolution orthophotos. Landsc Urban Plann 2003;63:1–14.
[88] Zinzi M, Agnoli S. Cool and green roofs. An energy and comfort comparison between passive cooling and mitigation urban heat island techniques for residential buildings in the Mediterranean region. Energy Build 2011;55:66–76.
[89] Bevilacqua P, Coma J, Pérez G, Chocarro C, Juárez A, Solé C, et al. Plant cover and floristic composition effect on thermal behaviour of extensive green roofs. Build Environ 2015;92:305–16. https://doi.org/10.1016/j.buildenv.2015.04.026.
[90] Mentens J, Raes D, Hermy M. Green roofs as a tool for solving the rainwater runoff problem in the urbanized 21st century? Landsc Urban Plann 2006;77: 217–26.
[91] Sfakianaki A, Pagalou E, Pavou K, Santamouris M, Assimakopoulos MN. Theoretical and experimental analysis of the thermal behaviour of a green roof system installed in two residential buildings in Athens, Greece. Int J Energy Res 2009;33:1059–69.
[92] Theodosiou T. Green roofs in buildings: thermal and environmental behaviour. Adv Build Energy Res 2009;3:271–88.
[93] La Roche P, Yeom DJ, Ponce A. Passive cooling with a hybrid green roof for extreme climates. Energy Build 2020;224:110243.
[94] Fachinello Krebs L, Johansson E. Influence of microclimate on the effect of green roofs in Southern Brazil – a study coupling outdoor and indoor thermal simulations. Energy Build 2021;241:110963.
[95] Hao X, Xing Q, Long P, Lin Y, Hu J, Tan H. Influence of vertical greenery systems and green roofs on the indoor operative temperature of air-conditioned rooms. J Build Eng 2020;31:101373.
[96] Kim J, Hong T, Jeong J, Koo C, Jeong K. An optimization model for selecting the optimal green systems by considering the thermal comfort and energy consumption. Appl Energy 2016;169:682–95.
[97] Cirrincione L, Marvuglia A, Scaccianoce G. Assessing the effectiveness of green roofs in enhancing the energy and indoor comfort resilience of urban buildings to climate change: methodology proposal and application. Build Environ 2021;205: 108198.
[98] Evangelisti L, Guattari C, Grazieschi G, Roncone M, Asdrubali F. On the energy performance of an innovative green roof in the Mediterranean climate. Energies 2020;13:5163.
[99] Chowdhury S, Hamada Y, Shabbir Ahmed K. Indoor heat stress and cooling energy comparison between green roof (GR) and non-green roof (n-GR) by simulations for labor intensive factories in the tropics. Int J Sustain Built Environ 2017;6:449–62.
[100] Pastore L, Corrao R, Heiselberg PK. The effects of vegetation on indoor thermal comfort: the application of a multi-scale simulation methodology on a residential neighborhood renovation case study. Energy Build 2017;146:1–11.
[101] Takakura T, Kitade S, Goto E. Cooling effect of greenery cover over a building. Energy Build 2000;31:1–6.
[102] Onmura S, Matsumoto M, Hokoi S. Study on evaporative cooling effect of roof lawn gardens. Energy Build 2001;33:653–66. https://doi.org/10.1016/S0378-7788(00)00134-1.
[103] Silva CM, Gomes MG, Silva M. Green roofs energy performance in Mediterranean climate. Energy Build 2016;116:318–25.
[104] Karachaliou P, Santamouris M, Pangalou H. Experimental and numerical analysis of the energy performance of a large scale intensive green roof system installed on an office building. Energy Build 2016;114:256–64.
[105] He Y, Yu H, Dong N, Ye H. Thermal and energy performance of extensive green roof in Summer: a case study of a lightweight building in Shanghai. Energy Build 2016;127:762–73.
[106] Squier M, Davidson CI. Heat flux and seasonal thermal performance of an external green roof. Build Environ 2016;107:235–44.
[107] Coma J, Perez G, Sole C, Castell A, Cabezza LF. Thermal assessment of extensive green roofs as passive tool for energy saving in buildings. Renew Energy 2016;85: 1106–15.
[108] Jiang L, Tang M. Thermal analysis of extensive green roofs combined with night ventilation for space cooling. Energy Build 2017;156:238–49.
[109] Bevilacqua P, Bruno R, Arcuri N. Green roofs in a Mediterranean climate: energy performance based on in-situ experimental data. Renew Energy 2020;152: 1414–30.
[110] Boafo FE, Kimb JT, Kim JH. Evaluating the impact of green roof evapotranspiration on annual building energy performance. Int J Og Green Energy 2017;14:479–89.
[111] Kokogiannakis G, Tietje A, Darkwa J. The role of green roofs on reducing heating and cooling loads: a database across Chinese Climates. Procedia Environ Sci 2011; 11:604–10.
[112] Kotsiris G, Androutsopoulos A, Polychroni E, Nektarios PA. Dynamic U-value estimation and energy simulation for green roofs. Energy Build 2012;45:240–9.
[113] Goussous J, Siam H, Alzoubi H. Prospects of green roof technology for energy and thermal benefits in buildings: case of Jordan. Sustain Cities Soc 2014;14:425–40.
[114] Virk G, Jansz A, Mavrogianni A, Mylona A, Stocker J, Davies M. Microclimate effects of green and cool roofs in London and their impacts on energy use for a typical office building. Energy Build 2015;88:214–28.
[115] Sharma A, Conry P, Fernando S, Hamlet AF, Hellmann JJ, Chen F. Green and cool roofs to mitigate urban heat island effects in the Chicago metropolitan area: evaluation with a regional climate model. Environ Res Lett 2016;11.
[116] Berardi U. The outdoor microclimate benefits and energy saving resulting from green roofs retrofits. Energy Build 2016;121:217–29.
[117] Ran J, Tang M. Effect of green roofs combined with ventilation on indoor cooling and energy consumption. Energy Proc 2017;141:260–6.
[118] Morakinyo TE, Dahanayake KWDK, Ng E, Chow CL. Temperature and cooling demand reduction by green-roof types in different climates and urban densities: a co-simulation parametric study. Energy Build 2017;145:226–37.
[119] He Y, Yu H, Ozaki A, Dong N. Thermal and energy performance of green and cool roof: a comparison study in Shanghai area. J Clean Prod 2020;267:122205.
[120] Polo-Labarrios MA, Quezada-Garcia S, Sancher-Mora H, Escobedo-Izquierdo MA, Espinosa-Paredes G. Comparison of thermal performance between green roofs and conventional roofs. Case Stud Therm Eng 2020;21:100697.
[121] Ávila-Hernández A, Simá E, Xamán J, Hernández-Pérez I, Téllez-Velázquez E, Chagolla-Aranda MA. Test box experiment and simulations of a green-roof: thermal and energy performance of a residential building standard for Mexico. Energy Build 2020;209:109709.
[122] Schade J, Lidelöw S, Lönnqvist J. The thermal performance of a green roof on a highly insulated building in a sub-arctic climate. Energy Build 2021;241:110961.
[123] Zheng X, Kong F, Yin H, Middel A, Liu H, Wang D, et al. Outdoor thermal performance of green roofs across multiple time scales: a case study in subtropical China. Sustain Cities Soc 2021;70:102909.
[124] Aboelata A. Assessment of green roof benefits on buildings' energy-saving by cooling outdoor spaces in different urban densities in arid cities. Energy 2021; 219:119514.
[125] Zhang K, Garg A, Mei G, Jiang M, Wang H, Huang S, et al. Thermal performance and energy consumption analysis of eight types of extensive green roofs in subtropical monsoon climate. Build Environ 2022;216:108982. https://doi.org/10.1016/j.buildenv.2022.108982.
[126] Beckett KP, Freer-Smith P, Taylor G. Urban woodlands: their role in reducing the effects of particulate pollution. Environ Pollut 1998;99:347–60.
[127] Kumar P, Druckman A, Gallagher J, Gatersleben B, Allison S, Eisenman TS, et al. The nexus between air pollution, green infrastructure and human health. Environ Int 2019;133.
[128] Benjamin MT, Sudol M, Bloch L, Winer AM. Low-emitting urban forests: a taxonomic methodology for assigning isoprene and monoterpene emission rates. Atmos Environ 1996;30:1437–52.
[129] Akbari H, Pomerantz M, Taha H. Cool surfaces and shade trees to reduce energy use and improve air quality in urban areas. Sol Energy 2001;70:295–310.
[130] Rosenfeld AH, Akbari H, Room JJ, Pomerantz M. Cool communities: strategies for heat island mitigation and smog reduction. Energy Build 1998;28:51–62.
[131] Nowak DJ. Air pollution removal by urban trees and shrubs in the United States. Urban For Urban Green 2006;4:115–23.
[132] Yang J, Yu Q, Gong P. Quantifying air pollution removal by green roofs in Chicago. Atmos Environ 2008;42:7266–73.
[133] Rowe DB. Green roofs as a means of pollution abatement. Environ Pollut 2011; 159:2100–10.
[134] Getter KL, Rowe DB, Robertson GP, Cregg BM, Andresen JA. Carbon sequestration potential of extensive green roofs. Environ Sci Technol 2009;43:7564–70.

[135] Baldocchi DD, Hicks BB, Camara P. A canopy stomatal resistance model for gaseous deposition to vegetated surfaces. Atmos Environ 1987;21:91–101.
[136] Tong Z, Whitlow TH, Landers A, Flanner B. A case study of air quality above an urban roof top vegetable farm. Environ Pollut 2016;208:256–60.
[137] Gourdji S. Review of plants to mitigate particulate matter, ozone as well as nitrogen dioxide air pollutants and applicable recommendations for green roofs in Montreal, Quebec. Environ Pollut 2018;241:378–87.
[138] Ramasubramanian P, Starry O, Rosenstiel T, Gall ET. Pilot study on the impact of green roofs on ozone levels near building ventilation air supply. Build Environ 2019;151:45–53.
[139] Currie BA, Bass B. Estimates of air pollution mitigation with green plants and green roofs using the UFORE model. Urban Ecosyst 2008;11:409–22.
[140] Xue MSX, Luo X. An overview of carbon sequestration of green roofs in urban areas. Urban For Urban Green 2020;47:126515.
[141] Li JF, Wai OWH, Li YS, Zhan JM, Ho YA, Li J, et al. Effect of green roof on ambient CO2 concentration. Build Environ 2010;45:2644–51.
[142] Heusinger J, Weber S. Extensive green roof CO2 exchange and its seasonal variation quantified by eddy covariance measurements. Sci Total Environ 2017;607–608:623–32.
[143] Luo H, Liu X, Anderson BC, Zhang K, Li X, Huang B, et al. Carbon sequestration potential of green roofs using mixed-sewagesludge substrate in Chengdu World Modern Garden City. Ecol Indicat 2015;49:247–59.
[144] Kuronuma T, Watanabe H, Ishihara T, Kou D, Toushima K, Ando M, et al. CO2 payoff of extensive green roofs with different vegetation species. Sustainability 2018;10.
[145] Olivares-Marin M, Maroto-Valer M. Development of adsorbents for CO2 capture from waste materials: a review. Greenhouse Gases Sci Technol 2012;2:20–35.
[146] Lei K-T, Tang J-S, Chen P-H. Numerical simulation and experiments with green roofs for increasing indoor thermal comfort. J Chin Inst Eng 2019;42:346–56. https://doi.org/10.1080/02533839.2019.1585207.
[147] Mutani G, Todeschi V. Roof-integrated green technologies, energy saving and outdoor thermal comfort: insights from a case study in urban environment. IJSDP 2021;16:13–23. https://doi.org/10.18280/ijsdp.160102.
[148] Wang X, Li H, Sodoudi S. The effectiveness of cool and green roofs in mitigating urban heat island and improving human thermal comfort. Build Environ 2022;217:109082. https://doi.org/10.1016/j.buildenv.2022.109082.
[149] Di Giuseppe E, D'Orazio M. Assessment of the effectiveness of cool and green roofs for the mitigation of the Heat Island effect and for the improvement of thermal comfort in Nearly Zero Energy Building. Architect Sci Rev 2015;58:134–43. https://doi.org/10.1080/00038628.2014.966050.
[150] Mutani G, Todeschi V. The effects of green roofs on outdoor thermal comfort, urban heat island mitigation and energy savings. Atmosphere 2020;11:123. https://doi.org/10.3390/atmos11020123.
[151] Ismail Asmat, Samad MHA, Rahman AMA. The investigation of green roof and white roof cooling potential on single storey residential building in the Malaysian climate. 2011. https://doi.org/10.5281/ZENODO.1330601.
[152] Ramasubramanian P, Luhung I, Lim SBY, Schuster SC, Starry O, Gall ET. Impact of green and white roofs on air handler filters and indoor ventilation air. Build Environ 2021;197:107860. https://doi.org/10.1016/j.buildenv.2021.107860.
[153] Lee JY, Moon HJ, Kim TI, Kim HW, Han MY. Quantitative analysis on the urban flood mitigation effect by the extensive green roof. Environ Pollut 2013;181:257–61.
[154] Lee JY, Lee MJ, Han M. A pilot study to evaluate runoff quantity from green roofs. J Environ Manag 2015;152:171–6.
[155] Vijayaraghavan K, Joshi UM, Balasubramanian R. A field study to evaluate runoff quality from green roofs. Water Res 2012;46:1337–45.
[156] Gong Y, Yin D, Li J, Zhang X, Wang W, Fang X, et al. Performance assessment of extensive green roof runoff flow and quality control capacity based on pilot experiments. Sci Total Environ 2019;687:505–15.
[157] Zhang S, Lin Z, Zhang S, Ge D. Stormwater retention and detention performance of green roofs with different substrates: observational data and hydrological simulations. J Environ Manag 2021:291.
[158] Liu W, Qian Y, Yao L, Feng Q, Engel BA, Chen W, et al. Identifying city-scale potential and priority areas for retrofitting green roofs and assessing their runoff reduction effectiveness in urban functional zones. J Clean Prod 2022;332:130064.
[159] Deutsch B, Whitlow H, Sullivan M, Savineau A. Re-greening. Proc. of 3rd North American green roof conference: greening rooftops for sustainable communities. Washington, DC: The Cardinal Group; 2005.
[160] Li WC, Yeung KKA. A comprehensive study of green roof performance from environmental perspective. Int J Sustain Built Environ 2014;3:127–34.
[161] Gregoire BG, Clausen JC. Effect of a modular extensive green roof on stormwater runoff and water quality. Ecol Eng 2011;37:963–9.
[162] Zhang Q, Miao L, Wangc X, Liu D, Zhu L, Zhou B, et al. The capacity of greening roof to reduce stormwater runoff and pollution. Landsc Urban Plann 2015;144:142–50.
[163] Liu W, Angel BA, Chen W, Wei W, Wang Y, Feng Q. Quantifying the contributions of structural factors on runoff water quality from green roofs and optimizing assembled combinations using Taguchi method. J Hydrol 2021;593:125864.
[164] Connelly M, Hodgson M. Experimental investigation of the sound transmission of vegetated roofs. Appl Acoust 2013;74:1136–43. https://doi.org/10.1016/j.apacoust.2013.04.003.
[165] Galbrun L, Scerri L. Sound insulation of lightweight extensive green roofs. Build Environ 2017;116:130–9. https://doi.org/10.1016/j.buildenv.2017.02.008.
[166] London A. The determination of reverberant sound absorption coefficients from acoustic impedance measurements. J Acoust Soc Am 1950;22:263–9. https://doi.org/10.1121/1.1906600.
[167] Horoshenkov KV, Khan A, Benkreira H. Acoustic properties of low growing plants. J Acoust Soc Am 2013;133:2554–65. https://doi.org/10.1121/1.4798671.
[168] Yang H-S, Kang J, Cheal C. Random-incidence absorption and scattering coefficients of vegetation. Acta Acustica United with Acustica 2013;99:379–88. https://doi.org/10.3813/AAA.918619.
[169] Brum R, Paul S, da Silva AR, Piovesan T. Acoustic absorption of green roof samples commercially available in southern Brazil. J Acoust Soc Am 2014;136:2305. https://doi.org/10.1121/1.4900338. 2305.
[170] Pittaluga I, Schenone C, Borelli D. Sound absorption of different green roof systems. J Acoust Soc Am 2011;130:2317. https://doi.org/10.1121/1.3654256. 2317.
[171] Connelly M, Hodgson M. Experimental investigation of the sound absorption characteristics of vegetated roofs. Build Environ 2015;92:335–46. https://doi.org/10.1016/j.buildenv.2015.04.023.
[172] Zwikker C, Kosten CW. Sound absorbing materials. Elsevier Pub. Co; 1949.
[173] Attenborough K. Acoustical impedance models for outdoor ground surfaces. J Sound Vib 1985;99:521–44. https://doi.org/10.1016/0022-460X(85)90538-3.
[174] Delany ME, Bazley EN. Acoustical properties of fibrous absorbent materials. Appl Acoust 1970;3:105–16. https://doi.org/10.1016/0003-682X(70)90031-9.
[175] Chessell CI. Propagation of noise along a finite impedance boundary. J Acoust Soc Am 1977;62:825–34. https://doi.org/10.1121/1.381603.
[176] Miki Y. Acoustical properties of porous materials. Modifications of Delany-Bazley models. J Acoust Soc Jpn E 1990;11:19–24. https://doi.org/10.1250/ast.11.19.
[177] Watanabe T, Yamada S. Sound attenuation through absorption by vegetation. J Acoust Soc Jpn E 1996;17:175–82. https://doi.org/10.1250/ast.17.175.
[178] Ding L, Van Renterghem T, Botteldooren D, Horoshenkov K, Khan A. Sound absorption of porous substrates covered by foliage: experimental results and numerical predictions. J Acoust Soc Am 2013;134:4599–609. https://doi.org/10.1121/1.4824830.
[179] Biot MA. Theory of propagation of elastic waves in a fluid-saturated porous solid. I. Low-Frequency range. J Acoust Soc Am 1956;28:168–78. https://doi.org/10.1121/1.1908239.
[180] Biot MA. Theory of propagation of elastic waves in a fluid-saturated porous solid. II. Higher frequency range. J Acoust Soc Am 1956;28:179–91. https://doi.org/10.1121/1.1908241.
[181] Horoshenkov KV, Mohamed MHA. Experimental investigation of the effects of water saturation on the acoustic admittance of sandy soils. J Acoust Soc Am 2006;120:1910–21. https://doi.org/10.1121/1.2338288.
[182] Horoshenkov KV, Khan A, Benkreira H. The effect of moisture and soil type on the acoustical properties of green noise controlelements. Denmark: Aalborg; 2011.
[183] Attal E, Haw G, Pot G, Vasseur C, Shimizu T, Granger C, et al. Experimental characterization of foliage and substrate samples by the three-microphone two-load method. INTER-NOISE and NOISE-CON Congress and Conference Proceedings, Hamburg GERMANY: [n.d].
[184] Oberhettinger F. Diffraction of waves by a wedge. Commun Pure Appl Math 1954;7:551–63. https://doi.org/10.1002/cpa.3160070306.
[185] Hadden WJ, Pierce AD. Sound diffraction around screens and wedges for arbitrary point source locations. J Acoust Soc Am 1981;69:1266–76. https://doi.org/10.1121/1.385809.
[186] Menounou P, Nikolaou P. An extension to the directive line source model for diffraction by half planes and wedges. Acta Acustica United with Acustica 2016;102:307–21. https://doi.org/10.3813/AAA.918947.
[187] Hewett DP, Morris A. Diffraction by a right-angled impedance wedge: an edge source formulation. J Acoust Soc Am 2015;137:633–9. https://doi.org/10.1121/1.4906265.
[188] Min H, Qiu X. Multiple acoustic diffraction around rigid parallel wide barriers. J Acoust Soc Am 2009;126:179–86. https://doi.org/10.1121/1.3147491.
[189] Menounou P, Asimakopoulos V. Empirical formulas for predicting the insertion loss behind wedges. Appl Acoust 2021;182:108166. https://doi.org/10.1016/j.apacoust.2021.108166.
[190] Yang HS, Kang J, Choi MS. Acoustic effects of green roof systems on a low-profiled structure at street level. Build Environ 2012;50:44–55. https://doi.org/10.1016/j.buildenv.2011.10.004.
[191] Van Renterghem T, Botteldooren D. In-situ measurements of sound propagating over extensive green roofs. Build Environ 2011;46:729–38. https://doi.org/10.1016/j.buildenv.2010.10.006.
[192] Van Renterghem T, Botteldooren D. Influence of rainfall on the noise shielding by a green roof. Build Environ 2014;82:1–8. https://doi.org/10.1016/j.buildenv.2014.07.025.
[193] Van Renterghem T, Botteldooren D. Numerical evaluation of sound propagating over green roofs. J Sound Vib 2008;317:781–99. https://doi.org/10.1016/j.jsv.2008.03.025.
[194] Van Renterghem T, Hornikx M, Forssen J, Botteldooren D. The potential of building envelope greening to achieve quietness. Build Environ 2013;61:34–44. https://doi.org/10.1016/j.buildenv.2012.12.001.
[195] El Bachawati M, Manneh R, Belarbi R, Dandres T, Nassab C, El Zakhem H. Cradle-to-gate Life Cycle Assessment of traditional gravel ballasted, white reflective, and vegetative roofs: a Lebanese case study. J Clean Prod 2016;137:833–42. https://doi.org/10.1016/j.jclepro.2016.07.170.
[196] Bozorg Chenani S, Lehvävirta S, Häkkinen T. Life cycle assessment of layers of green roofs. J Clean Prod 2015;90:153–62. https://doi.org/10.1016/J.JCLEPRO.2014.11.070.
[197] Gargari C, Bibbiani C, Fantozzi F, Campiotti CA. Environmental impact of green roofing: the contribute of a green roof to the sustainable use of natural resources in a life cycle approach. Agric Agric Sci Procedia 2016;8:646–56. https://doi.org/10.1016/j.aaspro.2016.02.087.

[198] Giama E, Papageorgiou C, Theodoridou I, Papadopoulos AM. Life cycle analysis and life cycle cost analysis of green roofs in the Mediterranean climatic conditions. Energy Sources, Part A 2021. https://doi.org/10.1080/15567036.2021.1914782.
[199] Koroxenidis E, Theodosiou T. Comparative environmental and economic evaluation of green roofs under Mediterranean climate conditions – extensive green roofs a potentially preferable solution. J Clean Prod 2021;311:127563. https://doi.org/10.1016/j.jclepro.2021.127563.
[200] Kotsiris G, Androutsopoulos A, Polychroni E, Souliotis M, Kavga A. Carbon footprint of green roof installation on school buildings in Greek Mediterranean climatic region. Int J Sustain Energy 2019;38:866–83. https://doi.org/10.1080/14786451.2019.1605992.
[201] Koura J, Manneh R, Belarbi R, El Khoury V, El Bachawati M. Comparative cradle to grave environmental life cycle assessment of traditional and extensive vegetative roofs: an application for the Lebanese context. Int J Life Cycle Assess 2020;25:423–42. https://doi.org/10.1007/s11367-019-01700-z.
[202] Tams L, Nehls T, Calheiros CSC. Rethinking green roofs- natural and recycled materials improve their carbon footprint. Build Environ 2022;219:109122. https://doi.org/10.1016/j.buildenv.2022.109122.
[203] Yao L, Chini A, Zeng R. Integrating cost-benefits analysis and life cycle assessment of green roofs: a case study in Florida. Hum Ecol Risk Assess 2020;26:443–58. https://doi.org/10.1080/10807039.2018.1514251.
[204] Rivela B, Cuerda I, Olivieri F, Bedoya C, Neila J. Life Cycle Assessment for ecodesign of ecological roof made with Intemper TF ecological water-tank system. Mater Construcción 2013;63. https://doi.org/10.3989/mc.2012.02611.
[205] Maiolo M, Carini M, Capano G, Piro P. Life cycle assessment (LCA) for water re use system of a green roof. Adv Mater Sci Eng 2018;2. https://doi.org/10.33140/amse/02/01/08.
[206] Sonetti G, Lombardi P. Multi-criteria decision analysis of a building element integrating energy use, environmental, economic and aesthetic parameters in its life cycle. Green Energy and Technology, Springer Verlag; 2020. p. 463–77. https://doi.org/10.1007/978-3-030-23786-8_26.
[207] Pushkar S. Modeling the substitution of natural materials with industrial byproducts in green roofs using life cycle assessments. J Clean Prod 2019;227:652–61. https://doi.org/10.1016/j.jclepro.2019.04.237.
[208] Maiolo M, Carini M, Capano G, Nigro G, Piro P. Life cycle assessment of a bitumen anti-root barrier on a green roof in the Mediterranean area. Int J Petrochem Res 2018;1:92–5. https://doi.org/10.18689/ijpr-1000116.
[209] Morau D, Rabarison T, Rakotondramiarana H. Life cycle analysis of green roof implemented in a global south low-income country. Br J Environ Clim Change 2017;7:43–55. https://doi.org/10.9734/bjecc/2017/30796.
[210] Vacek P, Struhala K, Matějka L. Life-cycle study on semi intensive green roofs. J Clean Prod 2017;154:203–13. https://doi.org/10.1016/j.jclepro.2017.03.188.
[211] I.S.O.. Environmental management - life cycle assessment - principles and framework. 2004. ISO 14040:2006.
[212] Peri G, Licciardi GR, Matera N, Mazzeo D, Cirrincione L, Scaccianoce G. Disposal of green roofs: a contribution to identifying an "Allowed by legislation" end–of–life scenario and facilitating their environmental analysis. Build Environ 2022;226:109739. https://doi.org/10.1016/j.buildenv.2022.109739.
[213] Ng E, Chen L, Wang Y, Yuan C. A study on the cooling effects of greening in a high-density city: an experience from Hong Kong. Build Environ 2012;47:256–71. https://doi.org/10.1016/j.buildenv.2011.07.014.
[214] Caneva G, Kumbaric A, Savo V, Casalini R. Ecological approach in selecting extensive green roof plants: a data-set of Mediterranean plants. Plant Biosyst 2015;149:374–83. https://doi.org/10.1080/11263504.2013.819819.
[215] Butler C, Butler E, Orians CM. Native plant enthusiasm reaches new heights: perceptions, evidence, and the future of green roofs. Urban For Urban Green 2012;11:1–10. https://doi.org/10.1016/j.ufug.2011.11.002.
[216] Blasi C, Marignani M, Copiz R, Fipaldini M, Bonacquisti S, Del Vico E, et al. Important plant areas in Italy: from data to mapping. Biol Conserv 2011;144:220–6. https://doi.org/10.1016/j.biocon.2010.08.019.
[217] Emilsson T, Czemiel Berndtsson J, Mattsson JE, Rolf K. Effect of using conventional and controlled release fertiliser on nutrient runoff from various vegetated roof systems. Ecol Eng 2007;29:260–71. https://doi.org/10.1016/j.ecoleng.2006.01.001.
[218] Suszanowicz D, Kolasa Więcek A. The impact of green roofs on the parameters of the environment in urban areas—review. Atmosphere 2019;10:792. https://doi.org/10.3390/atmos10120792.
[219] Monteiro CM, Calheiros CSC, Palha P, Castro PML. Growing substrates for aromatic plant species in green roofs and water runoff quality: pilot experiments in a Mediterranean climate. Water Sci Technol 2017;76:1081–9. https://doi.org/10.2166/wst.2017.276.
[220] IPCC. In: Pörtner H-O, Roberts DC, Tignor M, Poloczanska ES, Mintenbeck K, Alegría A, Craig M, Langsdorf S, Löschke S, Möller V, Okem A, Rama B, editors. Climate change 2022: impacts, adaptation and vulnerability. Contribution of working group II to the sixth assessment report of the intergovernmental panel on climate change. Cambridge, UK and New York, NY, USA: Cambridge University Press. Cambridge University Press; 2022. p. 3056. https://doi.org/10.1017/9781009325844.
[221] Pirouz B, Palermo SA, Turco M. Improving the efficiency of green roofs using atmospheric water harvesting systems (an innovative design). Water 2021;13:546. https://doi.org/10.3390/w13040546.
[222] Hosseinkhani O, Kargari A. Production of high-quality drinking water from chillers and air conditioning units' condensates using UV/GAC/MF/NF hybrid system. J Clean Prod 2022;368:133177. https://doi.org/10.1016/j.jclepro.2022.133177.